Heteroleptic Ter-bidentate Cr(III) Complexes as Tunable Optical Sensitizers

Benjamin Doistau,[*a] *Guillaume Collet,*[a,†] *Emilio Acuña Bolomey,*[a] *Vida Sadat-Noorbakhsh,*[a] *Céline Besnard,*[b] *and Claude Piguet**[a]

Supporting information

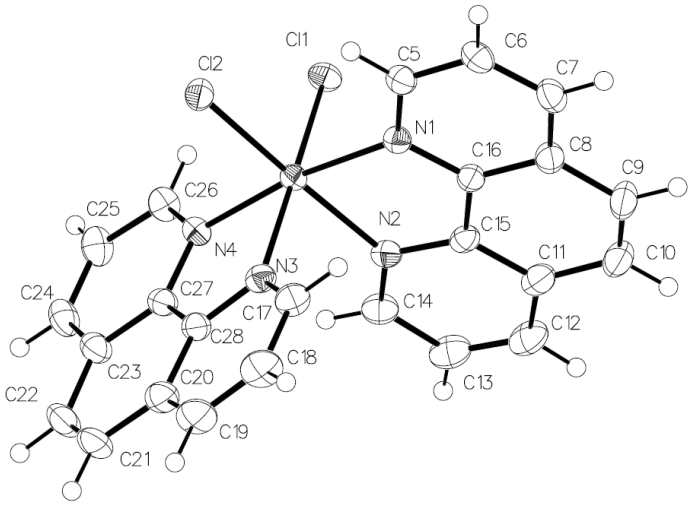

Fig. S1 Ortep view of $[Cr(phen)_2Cl_2]Cl$ $(CH_3)_2NCHO$ (**1**) with numbering scheme. Thermal ellipsoids are drawn at 50% probability level. Counter ions and solvent molecules are omitted for clarity.

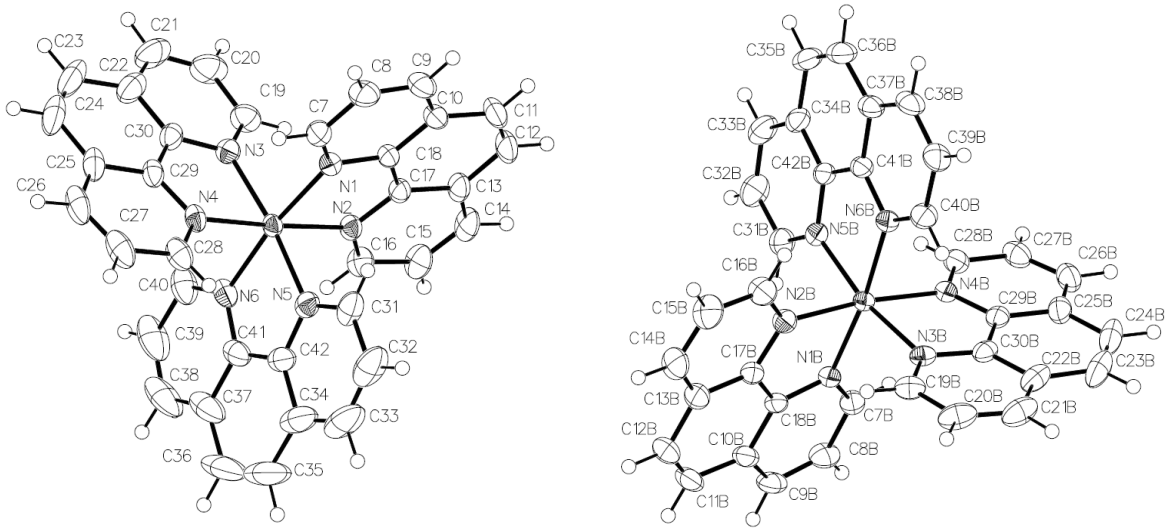

Fig. S2 Ortep views of $[Cr(phen)_3]_2(PF_6)_6$ $6.33CH_3CN$ (**2**) with numbering scheme showing the two asymmetric units. Thermal ellipsoids are drawn at 50% probability level. Counter ions and solvent molecules are omitted for clarity.

Table S1 Summary of crystal data, intensity measurements and structure refinements for $[Cr(phen)_2Cl_2]Cl$ $(CH_3)_2NCHO$ (**1**) and $[Cr(phen)_3]_2(PF_6)_6$ $6.33CH_3CN$ (**2**).

	$[Cr(phen)_2Cl_2]Cl$ $(CH_3)_2NCHO$ (**1**)	$[Cr(phen)_3]_2(PF_6)_6$ $6.33CH_3CN$ (**2**)
CCDC number	1865022	1865025
Empirical formula	$C_{27}H_{23}Cl_3CrN_5O$	$C_{84.69}H_{67.03}Cr_2F_{36}N_{18.35}P_6$
Formula weight	591.85 g/mol	2315.50 g/mol
Temperature	179.95(10) K	180.01(10) K
Radiation (Wavelength)	MoKα (λ = 0.71073 Å)	MoKα (λ = 0.71073 Å)
Crystal System, Space group	triclinc, *P*-1	monoclinc, $P2_1/c$
Unit cell dimensions	*a* = 8.3549(4) Å *b* = 10.1886(5) Å *c* = 15.3816(7) Å α = 94.630(4)° β = 93.725(4)° γ = 93.185(4)°	*a* = 35.6044(6) Å *b* = 16.9550(2) Å *c* = 15.9940(2) Å α = 90° β = 98.2157(14)° γ = 90°
Volume in $Å^3$	1299.89(11)	9556.0(2)
Z, Calculated density	2, 1.512 g/cm^3	4, 1.609 g/cm^3
Absorption coefficient	0.780 mm^{-1}	0.454 mm^{-1}
F(000)	606.0	4662.0
Crystal size (mm^3)	0.376 × 0.146 × 0.063	0.446 × 0.33 × 0.194
Theta range for data collection	3.071° to 29.261°	2.204° to 29.647°
Limiting indices	$-10 \le h \le 10$, $-14 \le k \le 11$, $-19 \le l \le 17$	$-37 \le h \le 49$, $-23 \le k \le 23$, $-22 \le l \le 22$
Reflections collected	9645	104247
Independent reflections	5949 [R_{int} = 0.0203, R_{sigma} = 0.0434]	24026 [R_{int} = 0.0300, R_{sigma} = 0.0285]
Data / restraints / parameters	5949/60/372	24026/303/1425
Goodness-of-fit on F^2	1.037	1.068
Final *R* indices [$I>2\sigma(I)$]	R_1 = 0.0425, wR_2 = 0.0997	R_1 = 0.0531, wR_2 = 0.1263
R indices (all data)	R_1 = 0.0551, wR_2 = 0.1101	R_1 = 0.0725, wR_2 = 0.1377
Largest diff. peak and hole	1.141/-0.641 e.$Å^{-3}$	0.839/-0.449 e.$Å^{-3}$

Table S2 Selected bond distances (Å), bond angles (°) in $[Cr(phen)_2Cl_2]Cl\ (CH_3)_2NCHO$ (**1**).

Bond distances (Å)			
Cr(1)-Cl(1)	2.2975(7)	Cr(1)-N(1)	2.0650(19)
Cr(1)-Cl(2)	2.2961(7)	Cr(1)-N(4)	2.0757(19)
Cr(1)-N(3)	2.085(2)	Cr(1)-N(2)	2.085(2)
Bond angles (°)			
Cl(2)-Cr(1)-Cl(1)	95.53(3)	N(4)-Cr(1)-Cl(1)	93.99(6)
N(3)-Cr(1)-Cl(1)	172.42(6)	N(4)-Cr(1)-Cl(2)	91.82(6)
N(3)-Cr(1)-Cl(2)	88.83(6)	N(4)-Cr(1)-N(3)	79.64(8)
N(1)-Cr(1)-Cl(1)	90.04(6)	N(4)-Cr(1)-N(2)	93.35(8)
N(1)-Cr(1)-Cl(2)	94.47(6)	N(2)-Cr(1)-Cl(1)	88.00(6)
N(1)-Cr(1)-N(3)	95.82(8)	N(2)-Cr(1)-Cl(2)	173.52(6)
N(1)-Cr(1)-N(4)	172.18(8)	N(2)-Cr(1)-N(3)	88.27(8)
N(1)-Cr(1)-N(2)	80.07(8)		

Table S3 Selected bond distances (Å), bond angles (°) in $[Cr(phen)_3](PF_6)_6\ 6.33CH_3CN$ (**2**).

Bond distances (Å)			
Cr(1)-N(1)	2.0566(19)	Cr(1)-N(4)	2.0418(18)
Cr(1)-N(2)	2.0642(19)	Cr(1)-N(5)	2.047(2)
Cr(1)-N(3)	2.041(2)	Cr(1)-N(6)	2.042(2)
Cr(1B)-N(1B)	2.0495(17)	Cr(1B)-N(4B)	2.0551(19)
Cr(1B)-N(2B)	2.0460(19)	Cr(1B)-N(3B)	2.0498(19)
Cr(1B)-N(5B)	2.0520(19)	Cr(1B)-N(6B)	2.0638(18)
Bond angles (°)			
N(1)-Cr(1)-N(2)	80.85(8)	N(4)-Cr(1)-N(5)	94.01(8)
N(3)-Cr(1)-N(1)	90.95(8)	N(4)-Cr(1)-N(6)	88.97(8)
N(3)-Cr(1)-N(2)	96.50(8)	N(5)-Cr(1)-N(1)	94.13(8)
N(3)-Cr(1)-N(4)	81.31(8)	N(5)-Cr(1)-N(2)	88.34(8)
N(3)-Cr(1)-N(5)	173.49(8)	N(6)-Cr(1)-N(1)	172.61(8)
N(3)-Cr(1)-N(6)	94.27(9)	N(6)-Cr(1)-N(2)	93.34(8)
N(4)-Cr(1)-N(1)	97.00(8)	N(6)-Cr(1)-N(5)	81.06(9)

N(4)-Cr(1)-N(2)	176.93(8)		
N(1B)-Cr(1B)-N(5B)	94.53(7)	N(2B)-Cr(1B)-N(6B)	94.39(8)
N(1B)-Cr(1B)-N(4B)	95.34(7)	N(5B)-Cr(1B)-N(4B)	92.95(7)
N(1B)-Cr(1B)-N(3B)	94.15(7)	N(5B)-Cr(1B)-N(6B)	81.03(7)
N(1B)-Cr(1B)-N(6B)	173.36(7)	N(4B)-Cr(1B)-N(6B)	89.84(7)
N(2B)-Cr(1B)-N(1B)	80.82(7)	N(3B)-Cr(1B)-N(5B)	169.84(7)
N(2B)-Cr(1B)-N(5B)	92.66(8)	N(3B)-Cr(1B)-N(4B)	80.98(8)
N(2B)-Cr(1B)-N(4B)	173.44(8)	N(3B)-Cr(1B)-N(6B)	90.76(7)
N(2B)-Cr(1B)-N(3B)	93.93(8)		

Table S4 Interplanar angles (°) in $[Cr(phen)_2Cl_2]Cl$ $(CH_3)_2NCHO$ (**1**).

Phen1 N1 C5 C6 C7 C8 C9 C10 C11 C12 C13 C14 N2 C15 C16

Phen2 N3 C17 C18 C19 C20 C21 C22 C23 C24 C25 C26 N4 C27 C28

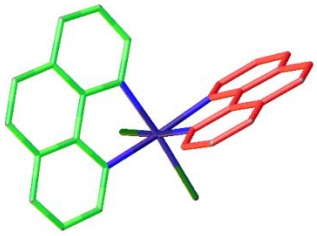

	Phen1
Phen2	90.1°

The error is typically ±0.1°.

Table S5 Interplanar angles (°) in $[Cr(phen)_3](PF_6)_6$ 6.33CH_3CN (**2**).

Phen1 N1 C7 C8 C9 C10 C11 C12 C13 C14 C15 C16 N2 C17 C18

N1B C7B C8B C9B C10B C11B C12B C13B C14B C15B C16B N2B C17B C18B

Phen2 N3 C19 C20 C21 C22 C23 C24 C25 C26 N4 C27 C28 C29 C30

N3B C19B C20B C21B C22B C23B C24B C25B C26B N4B C27B C28B C29B C30B

Phen3 N6B C40 C39 C38 C37 C36 C35 C34N C33 C32 C31 N5 C42 C41

N6B C40B C39B C38B C37B C36B C35B C34N C33B C32B C31B N5B C42B C41B

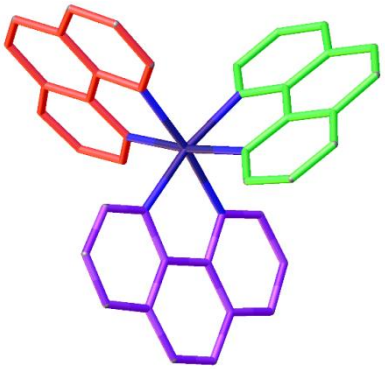

	Phen2	Phen3
Phen1	88.74°	92.357°
Phen2		81.73°

B	Phen2	Phen3
Phen1	80.583°	85.83°
Phen2		83.23°

The error is typically ±0.1°.

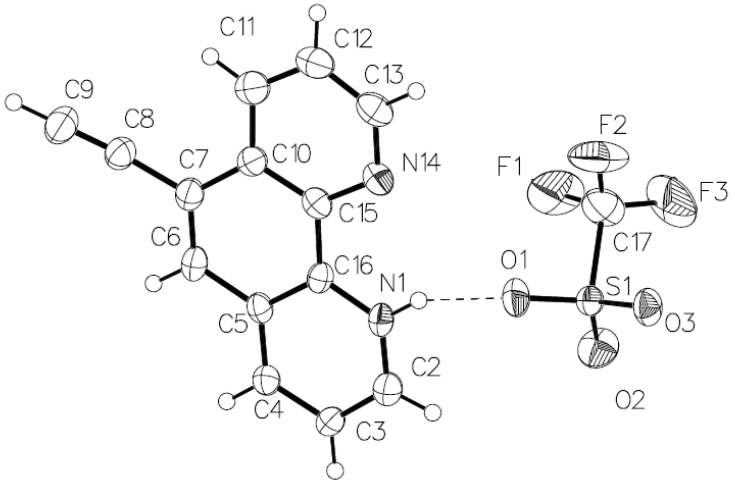

Fig. S3 Ortep views of (phenAlkynH)(CF_3SO_3) (**4**) with numbering scheme. Thermal ellipsoids are drawn at 50% probability level.

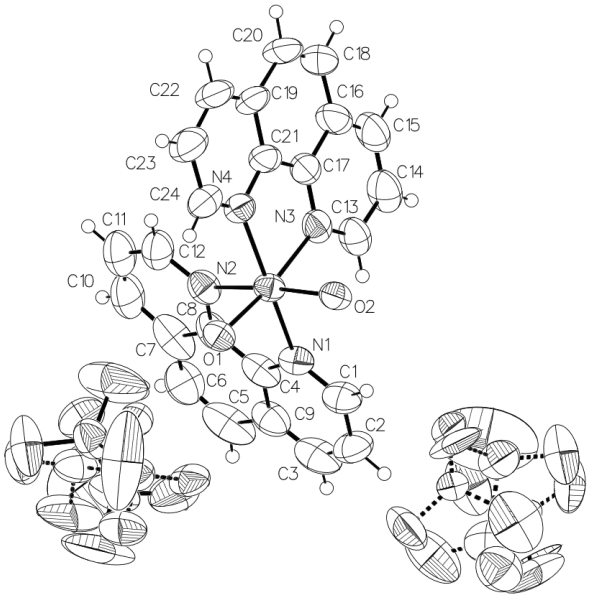

Fig. S4 Ortep views of $[Cr(phen)_2(H_2O)(OH)](CF_3SO_3)_2$ (**5**) with numbering scheme. Thermal ellipsoids are drawn at 50% probability level. Attempts to refine the structure of $[Cr(phen)_2(H_2O)(OH)](SO_3CF_3)_2$ (**5**) were unsatisfactory. The structure is twinned (twin law -1 0 0 0 -1 0 1 0 1) and we observed a superstructure with modulation along a and c axis. The best refinement obtained, without considering the modulation gives the average structure shown in Figure S4 and confirms the structure of the complex. However, more processing needs to be done to obtain a satisfactory crystal structure. There are two triflate anions per complex molecule. The bond valence sum (calculated to be 2.93) confirms that the oxidation number of the chromium is 3. One of the oxygen atom linked to the chromium atom must belong to a hydroxide anion and one to a water molecule. The quality of the structure does not allow to see such fine details and the hydrogen were not added to the water and hydroxide molecules.

Table S6 Summary of crystal data, intensity measurements and structure refinements for (phenAlkynH)(CF_3SO_3) (**4**) and [Cr(phen)$_2$(H_2O)(OH)](CF_3SO_3)$_2$ (**5**).

	(phenAlkynH)(SO_3CF_3) (**4**)	[Cr(phen)$_2$(H_2O)(OH)](SO_3CF_3)$_2$ (**5**)
CCDC number	1865017	Not deposited (see caption S4)
Empirical formula	$C_{15}H_9F_3N_2O_3S$	$C_{26}H_{16}CrF_6N_4O_8S_2$
Formula weight	354.30 g/mol	742.55 g/mol
Temperature	180.00(10) K	180.00(10) K
Radiation (Wavelength)	CuKα (λ = 1.54184 Å)	CuKα (λ = 1.54184 Å)
Crystal System, Space group	monoclinic, *C*2	monoclinc, *I* 2/a
Unit cell dimensions	*a* = 16.4058(3) Å *b* = 8.2898(2) Å *c* = 10.9282(2) Å α = 90° β = 90.184(2)° γ = 90°	*a* = 16.3908(4) Å *b* = 16.1562(3) Å *c* = 24.8931(7) Å α = 90° β = 109.154(3)° γ = 90°
Volume in Å^3	1486.24(5)	6227.1(3)
Z, Calculated density	4, 1.583 g/cm^3	8, 1.584 g/cm^3
Absorption coefficient	2.443 mm^{-1}	5.100 mm^{-1}
F(000)	720.0	2992
Crystal size (mm^3)	0.622 × 0.172 × 0.069	0.206 × 0.199 × 0.036
Theta range for data collection	8.09° to 147.374°	3.319° to 73.791°
Limiting indices	-20 ≤ *h* ≤ 19, -9 ≤ *k* ≤ 10, -13 ≤ *l* ≤ 12	-19 ≤ *h* ≤ 20, -20 ≤ *k* ≤ 19, -30 ≤ *l* ≤ 30
Reflections collected	8582	22072
Independent reflections	2801 [R_{int} = 0.0313, R_{sigma} = 0.0239]	6210 [R_{int} = 0.0247]
Data / restraints / parameters	2801/1/221	6210/228/499
Goodness-of-fit on F^2	1.134	1.429
Final *R* indices [$I>2\sigma(I)$]	R_1 = 0.0444, wR_2 = 0.1207	R_1 = 0.1039, wR_2 = 0.3044
R indices (all data)	R_1 = 0.0448, wR_2 = 0.1209	R_1 = 0.1190, wR_2 = 0.3295
Largest diff. peak and hole	0.24/-0.28 e.Å^{-3}	1.653/-0.808 e.Å^{-3}
Flack parameter	0.08(4)	

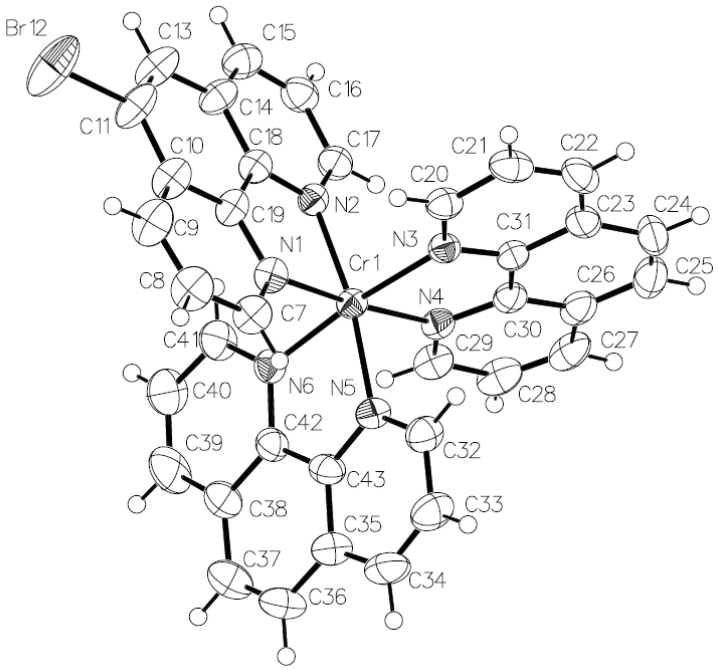

Fig. S5 Ortep views of $[Cr(phen)_2(phenBr)](PF_6)_3$ $2CH_3CN$ (**3**) with numbering scheme. Thermal ellipsoids are drawn at 50% probability level. Counter ions and solvent molecules are omitted for clarity.

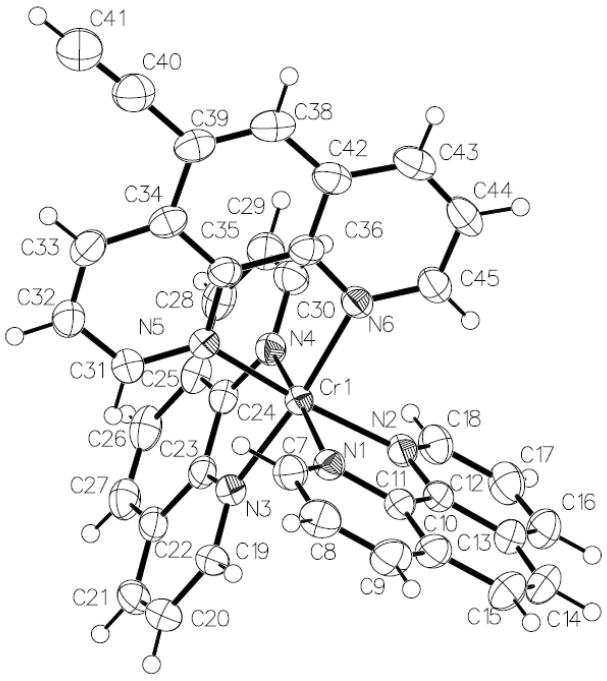

Fig. S6 Ortep views of $[Cr(phen)_2(phenAlkyn)](BF_4)_3$ $2CH_3CN$ (**6**) with numbering scheme. Thermal ellipsoids are drawn at 50% probability level. Counter ions and solvent molecules are omitted for clarity.

Table S7 Summary of crystal data, intensity measurements and structure refinements for $[Cr(phen)_2(phenBr)](PF_6)_3\ 2CH_3CN$ (**3**) and $[Cr(phen)_2(phenAlkyn)](BF_4)_3\ 2CH_3CN$ (**6**).

	$[Cr(phen)_2(phenBr)](PF_6)_3\ 2CH_3CN$ (**3**)	$[Cr(phen)_2(phenAlkyn)](BF_4)_3\ 2CH_3CN$ (**6**)
CCDC number	1865021	1865018
Empirical formula	$C_{40}H_{29}BrCrF_{18}N_8P_3$	$C_{42}H_{30}B_3CrF_{12}N_8$
Formula weight	1188.53g/mol	959.17 g/mol
Temperature	180.00(10) K	180.01(10) K
Radiation (Wavelength)	MoKα (λ = 0.71073 Å)	CuKα (λ = 1.54184 Å)
Crystal System, Space group	triclinc, *P*-1	triclinic, *P*-1
Unit cell dimensions	*a* = 13.0523(11) Å *b* = 13.6628(10) Å *c* = 14.4982(13) Å α = 85.468(7)° β = 78.983(7)° γ = 76.627(7)°	*a* = 9.8718(4) Å *b* = 11.2190(5) Å *c* = 19.1064(7) Å α = 78.995(3)° β = 80.846(3)° γ = 79.533(3)°
Volume in Å^3	2467.4(4)	2025.57(14)
Z, Calculated density	2, 1.600 g/cm^3	2, 1.573 g/cm^3
Absorption coefficient	1.246 mm^{-1}	3.217 mm^{-1}
F(000)	1182.0	970.0
Crystal size (mm^3)	0.908 × 0.291 × 0.174	0.708 × 0.133 × 0.057
Theta range for data collection	1.976° to 29.344°	4.064° to 73.557°
Limiting indices	$-17 \le h \le 17$, $-17 \le k \le 18$, $-18 \le l \le 16$	$-8 \le h \le 11$, $-12 \le k \le 13$, $-22 \le l \le 23$
Reflections collected	20866	13719
Independent reflections	11393 [R_{int} = 0.0291, R_{sigma} = 0.0519]	7904 [R_{int} = 0.0216, R_{sigma} = 0.0348]
Data / restraints / parameters	11393/0/642	7904/72/637
Goodness-of-fit on F^2	1.042	1.039
Final *R* indices [$I>2\sigma(I)$]	R_1 = 0.0769, wR_2 = 0.2111	R_1 = 0.0562, wR_2 = 0.1620
R indices (all data)	R_1 = 0.1150, wR_2 = 0.2443	R_1 = 0.0605, wR_2 = 0.1670
Largest diff. peak and hole	2.245/-1.494 e.Å^{-3}	0.729/-0.685 e.Å^{-3}

Table S8 Selected bond distances (Å), bond angles (°) in $[Cr(phen)_2(phenBr)](PF_6)_3$ $2CH_3CN$ (**3**).

Bond distances (Å)			
Cr(1)-N(1)	2.063(4)	Cr(1)-N(4)	2.060(4)
Cr(1)-N(2)	2.038(3)	Cr(1)-N(5)	2.054(4)
Cr(1)-N(3)	2.058(3)	Cr(1)-N(6)	2.057(4)
Bond angles (°)			
N(2)-Cr(1)-N(1)	80.80(15)	N(5)-Cr(1)-N(1)	94.01(15)
N(2)-Cr(1)-N(3)	90.70(14)	N(5)-Cr(1)-N(3)	96.83(15)
N(2)-Cr(1)-N(4)	97.25(15)	N(5)-Cr(1)-N(4)	88.47(15)
N(2)-Cr(1)-N(5)	171.22(15)	N(5)-Cr(1)-N(6)	80.55(15)
N(2)-Cr(1)-N(6)	92.48(15)	N(6)-Cr(1)-N(1)	91.87(15)
N(3)-Cr(1)-N(1)	95.02(15)	N(6)-Cr(1)-N(3)	172.80(15)
N(3)-Cr(1)-N(4)	80.53(15)	N(5)-Cr(1)-N(1)	94.01(15)
N(4)-Cr(1)-N(1)	175.15(15)		

Table S9 Selected bond distances (Å), bond angles (°) in $[Cr(phen)_2(phenAlkyn)](BF_4)_3$ $2CH_3CN$ (**6**).

Bond distances (Å)			
Cr(1)-N(1)	2.050(2)	Cr(1)-N(4)	2.051(2)
Cr(1)-N(2)	2.047(2)	Cr(1)-N(5)	2.064(2)
Cr(1)-N(3)	2.054(2)	Cr(1)-N(6)	2.062(2)
Bond angles (°)			
N(1)-Cr(1)-N(3)	93.62(9)	N(2)-Cr(1)-N(6)	93.12(9)
N(1)-Cr(1)-N(4)	172.75(9)	N(3)-Cr(1)-N(5)	94.45(8)
N(1)-Cr(1)-N(5)	94.76(8)	N(3)-Cr(1)-N(6)	173.67(9)
N(1)-Cr(1)-N(6)	90.45(8)	N(4)-Cr(1)-N(3)	80.91(9)
N(2)-Cr(1)-N(1)	81.21(9)	N(4)-Cr(1)-N(5)	90.42(9)
N(2)-Cr(1)-N(3)	92.30(8)	N(4)-Cr(1)-N(6)	95.42(9)
N(2)-Cr(1)-N(4)	94.21(9)	N(6)-Cr(1)-N(5)	80.37(9)
N(2)-Cr(1)-N(5)	172.35(8)		

Table S10 Interplanar angles (°) in $[Cr(phen)_2(phenBr)](PF_6)_3$ $2CH_3CN$ (**3**).

Phen1 C13 C11 C10 C9 C8 C7 N1 C19 C18 C14 C15 C16 N2 C17

Phen2 C20 C21 C22 C23 C24 C25 C26 C30 C31 C27 C28 C29 N4 N3

Phen3 N5 C32 C33 C34 C35 C43 N6 C42 C41 C40 C39 C38 C37 C36

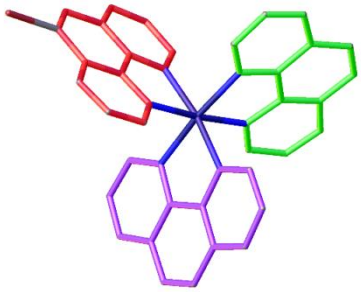

	Phen2	Phen3
Phen1	86.7°	91.4°
Phen2		97.6°

The error is typically ±0.1°.

Table S11 Interplanar angles (°) in $[Cr(phen)_2(phenAlkyn)](BF_4)_3$ $2CH_3CN$ (**6**).

Phen1 N1 C7 C8 C9 C10 C11 C12 C13 C14 C15 C16 N2 C17 C18

Phen2 N3 C19 C20 C21 C22 C23 C24 C25 C26 N4 C27 C28 C29 C30

Phen3 N6B C40 C39 C38 C37 C36 C35 C34 C33 C32 C31 N5 C42 C41 C43 C44

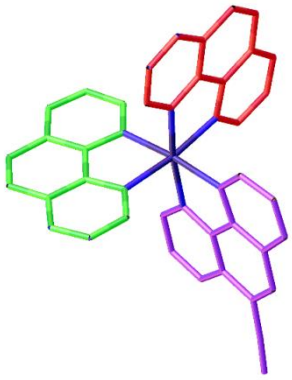

	Phen2	Phen3
Phen1	93.6°	91.7°
Phen2		94.4°

The error is typically ±0.1°.

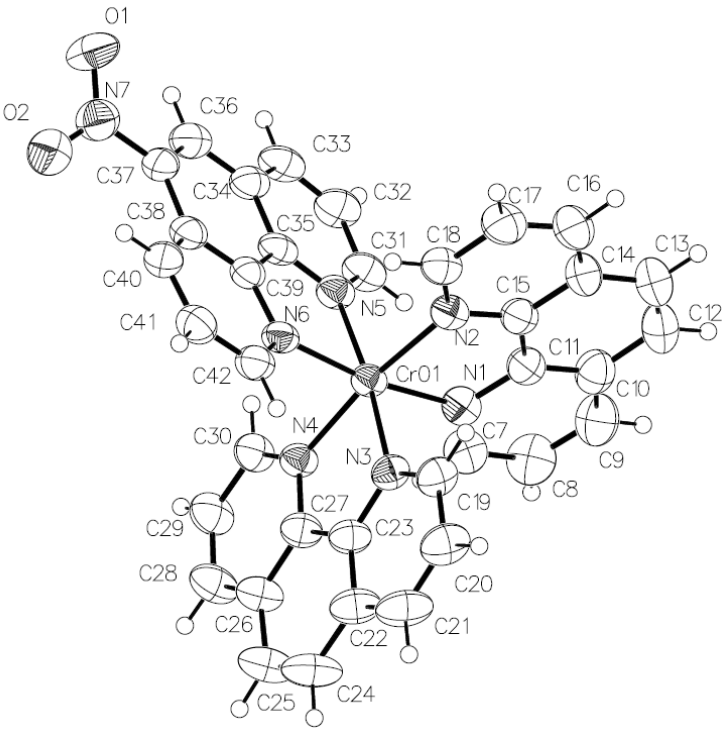

Fig. S7 Ortep views of $[Cr(phen)_2(phenNO_2)](CF_3SO_3)_3$ (**7**) with numbering scheme. Thermal ellipsoids are drawn at 50% probability level. Counter ions and solvent molecules are omitted for clarity.

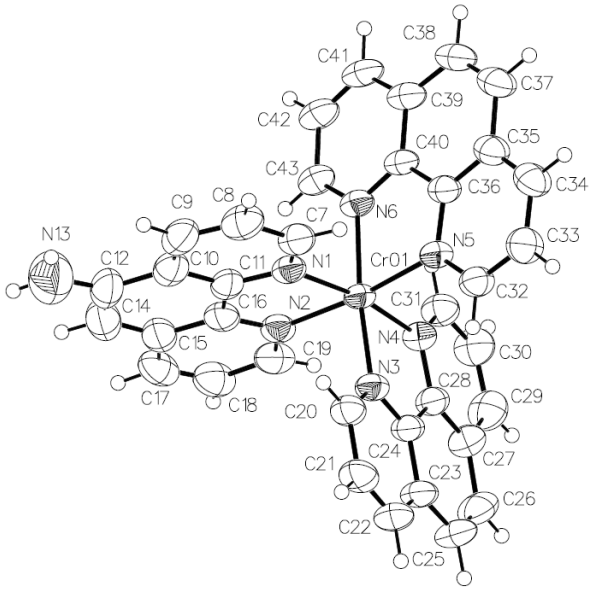

Fig. S8 Ortep views of $[Cr(phen)_2(phenNH_2)](CF_3SO_3)_3$ $1.83CH_3CN$ (**8**) with numbering scheme. Thermal ellipsoids are drawn at 50% probability level. Counter ions and solvent molecules are omitted for clarity.

Table S12 Summary of crystal data, intensity measurements and structure refinements for $[Cr(phen)_2(phenNO_2)](CF_3SO_3)_3$ (**7**) and $[Cr(phen)_2(phenNH_2)](CF_3SO_3)_3$ $1.83CH_3CN$ (**8**).

	$[Cr(phen)_2(phenNO_2)](SO_3CF_3)_3$ (**7**)	$[Cr(phen)_2(phenNH_2)](SO_3CF_3)_3$ $1.83CH_3CN$ (**8**)
CCDC number	1865020	1865019
Empirical formula	$C_{39}H_{23}CrF_9N_7O_{11}S_3$	$C_{42.64}H_{30.47}CrF_9N_{8.82}O_9S_3$
Formula weight	1084.82g/mol	1129.62 g/mol
Temperature	180.00(10) K	180.02(10) K
Radiation (Wavelength)	CuKα (λ = 1.54184 Å)	CuKα (λ = 1.54184 Å)
Crystal System, Space group	monoclinc, $P2_1/c$	triclinic, P-1
Unit cell dimensions	a = 14.0094(3) Å b = 13.2631(2) Å c = 27.2016(5) Å α = 90° β = 90.4760(19)° γ = 90°	a = 13.0266(3) Å b = 13.0574(3) Å c = 14.2638(3) Å α = 93.8354(17)° β = 99.1121(17)° γ = 96.6980(17)°
Volume in $Å^3$	5054.13(16)	2370.18(9)
Z, Calculated density	4, 1.426 g/cm^3	2, 1.583 g/cm^3
Absorption coefficient	3.860 mm^{-1}	4.118 mm^{-1}
F(000)	2188.0	1146.0
Crystal size (mm^3)	0.433 × 0.146 × 0.08	0.511 × 0.252 × 0.044
Theta range for data collection	3.155° to 66.601°	3.150° to 73.740°
Limiting indices	$-16 \le h \le 16$, $-15 \le k \le 15$, $-32 \le l \le 31$	$-16 \le h \le 16$, $-16 \le k \le 15$, $-17 \le l \le 17$
Reflections collected	37654	34290
Independent reflections	8922 [R_{int} = 0.0341, R_{sigma} = 0.0260]	9423 [R_{int} = 0.0635, R_{sigma} = 0.0451]
Data / restraints / parameters	8922/0/638	9423/9/670
Goodness-of-fit on F^2	1.034	1.042
Final R indices [$I>2\sigma(I)$]	R_1 = 0.0671, wR_2 = 0.1971	R_1 = 0.0780, wR_2 = 0.2325
R indices (all data)	R_1 = 0.0715, wR_2 = 0.2023	R_1 = 0.0867, wR_2 = 0.2461
Largest diff. peak and hole	1.391/-0.818 e.Å^{-3}	1.431/-1.015 e.Å^{-3}

Table S13 Selected bond distances (Å), bond angles (°) in $[Cr(phen)_2(phenNO_2)](CF_3SO_3)_3$ (**7**).

Bond distances (Å)			
Cr(1)-N(1)	2.055(3)	Cr(1)-N(4)	2.046(3)
Cr(1)-N(2)	2.047(3)	Cr(1)-N(5)	2.046(3)
Cr(1)-N(3)	2.050(3)	Cr(1)-N(6)	2.054(3)
Bond angles (°)			
N(2)-Cr(1)-N(1)	81.25(12)	N(4)-Cr(1)-N(6)	92.20(12)
N(2)-Cr(1)-N(3)	93.39(12)	N(5)-Cr(1)-N(1)	91.98(13)
N(2)-Cr(1)-N(6)	93.36(12)	N(5)-Cr(1)-N(2)	91.43(11)
N(3)-Cr(1)-N(1)	92.49(12)	N(5)-Cr(1)-N(3)	173.88(12)
N(3)-Cr(1)-N(6)	95.03(11)	N(5)-Cr(1)-N(4)	94.57(11)
N(4)-Cr(1)-N(1)	93.86(12)	N(5)-Cr(1)-N(6)	80.91(12)
N(4)-Cr(1)-N(2)	172.40(12)	N(6)-Cr(1)-N(1)	171.00(12)
N(4)-Cr(1)-N(3)	80.95(12)		

Table S14 Selected bond distances (Å), bond angles (°) in $[Cr(phen)_2(phenNH_2)](CF_3SO_3)_3$ $1.83CH_3CN$ (**8**).

Bond distances (Å)			
Cr(1)-N(1)	2.054(3)	Cr(1)-N(4)	2.038(3)
Cr(1)-N(2)	2.062(3)	Cr(1)-N(5)	2.056(3)
Cr(1)-N(3)	2.049(3)	Cr(1)-N(6)	2.062(3)
Bond angles (°)			
N(1)-Cr(1)-N(2)	81.09(13)	N(4)-Cr(1)-N(2)	90.64(13)
N(1)-Cr(1)-N(5)	95.31(12)	N(4)-Cr(1)-N(3)	81.24(12)
N(1)-Cr(1)-N(6)	89.62(12)	N(4)-Cr(1)-N(5)	93.38(12)
N(3)-Cr(1)-N(1)	93.51(12)	N(4)-Cr(1)-N(6)	96.35(12)
N(3)-Cr(1)-N(2)	90.80(12)	N(5)-Cr(1)-N(2)	173.80(12)
N(3)-Cr(1)-N(5)	94.47(12)	N(5)-Cr(1)-N(6)	80.39(12)
N(3)-Cr(1)-N(6)	174.22(12)	N(6)-Cr(1)-N(2)	94.49(12)
N(4)-Cr(1)-N(1)	170.18(13)		

Table S15 Interplanar angles (°) in $[Cr(phen)_2(phenNO_2)](CF_3SO_3)_3$ (**7**).

Phen1 N1 C7 C8 C9 C10 C11 C15 N2 C18 C17 C16 C14 C13 C12

Phen2 N3 C19 C20 C21 C22 C23 C27 C26 C25 C24 C28 C29 C30 N4

Phen3 N5 C41 C42 C38 C40 C39 C35 C31 C32 C33 C34 C36 C37 N6

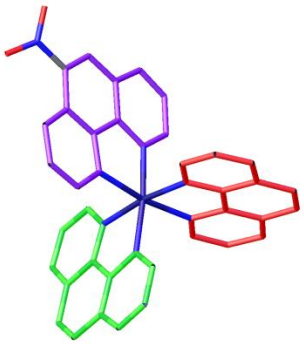

	Phen2	Phen3
Phen1	86.4°	88.5°
Phen2		84.9°

The error is typically ±0.1°.

Table S16 Interplanar angles (°) in $[Cr(phen)_2(phenNH_2)](CF_3SO_3)_3$ 1.83CH_3CN (**8**).

Phen1 C31 N4 C28 C24 N3 C20 C21 C22 C23 C25 C26 C27 C29 C30

Phen2 C43 C42 C41 C39 C40 C36 C35 C38 C37 C34 C33 C32 N5

Phen3 C7 N1 C11 C8 C9 C10 C12 C14 C15 C16 N2 C19 C18 C17

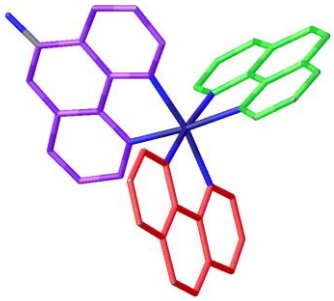

	Phen2	Phen3
Phen1	99.8°	87.4°
Phen2		85.6°

The error is typically ±0.1°.

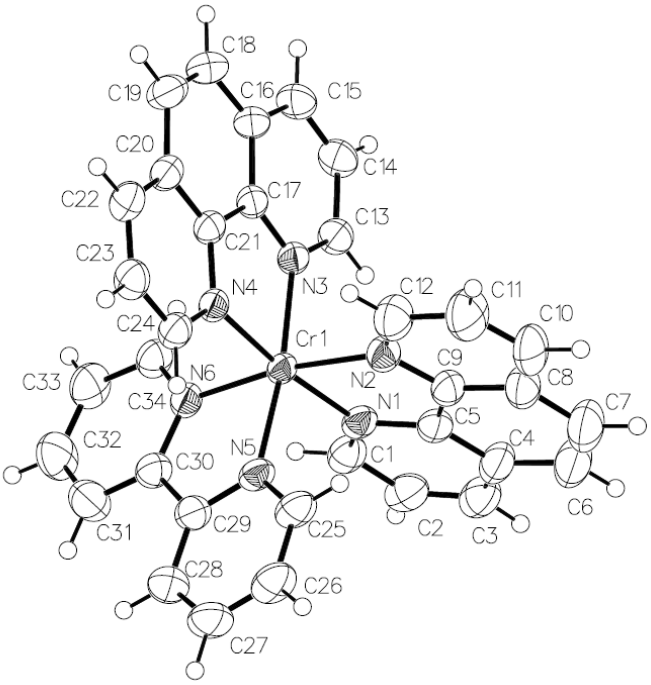

Fig. S9 Ortep views of $[Cr(phen)_2(bipy)](CF_3SO_3)_3$ (**9**) with numbering scheme. Thermal ellipsoids are drawn at 50% probability level. Counter ions and solvent molecules are omitted for clarity.

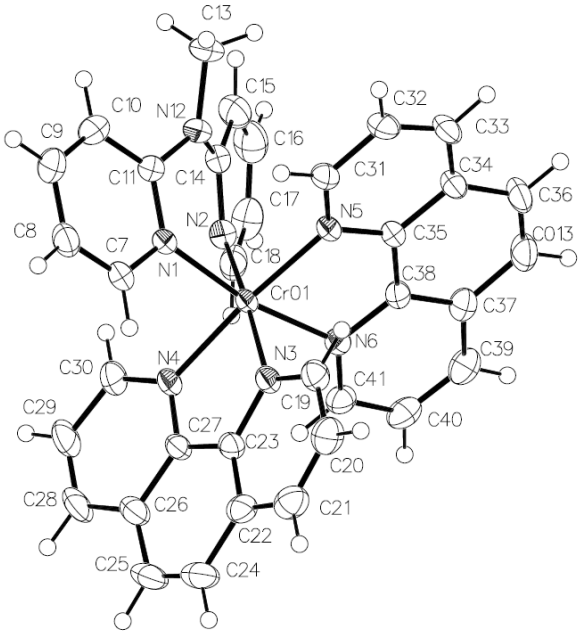

Fig. S10 Ortep views of $[Cr(phen)_2(dpma)](CF_3SO_3)_3$ (**10**) with numbering scheme. Thermal ellipsoids are drawn at 50% probability level. Counter ions and solvent molecules are omitted for clarity.

Table S17 Summary of crystal data, intensity measurements and structure refinements for $[Cr(phen)_2(bipy)](CF_3SO_3)_3$ (**9**) and $[Cr(phen)_2(dpma)](CF_3SO_3)_3$ (**10**).

	$[Cr(phen)_2(bipy)](SO_3CF_3)_3$ (**9**)	$[Cr(phen)_2(dpma)](SO_3CF_3)_3$ (**10**)
CCDC number	1865024	1865023
Empirical formula	$C_{37}H_{24}CrF_9N_6O_9S_3$	$C_{38}H_{27}CrF_9N_7O_9S_3$
Formula weight	1015.80 g/mol	1044.84 g/mol
Temperature	180.00(10) K	180.00(10) K
Radiation (Wavelength)	CuKα (λ = 1.54184 Å)	CuKα (λ = 1.54184 Å)
Crystal System, Space group	triclinc, *P*-1	triclinic, *P*-1
Unit cell dimensions	*a* = 12.9381(6) Å *b* = 13.5100(6) Å *c* = 17.6177(7) Å α = 101.751(4)° β = 97.407(4)° γ = 112.946(4)°	*a* = 10.7638(4) Å *b* = 13.0689(5) Å *c* = 15.5839(5) Å α = 72.716(3)° β = 87.940(3)° γ = 82.460(3)°
Volume in Å^3	2701.2(2)	2075.11(14)
Z, Calculated density	2, 1.249 g/cm^3	2, 1.672 g/cm^3
Absorption coefficient	3.540 mm^{-1}	4.633 mm^{-1}
F(000)	1026.0	1058.0
Crystal size (mm^3)	0.215 × 0.105 × 0.053	0.407 × 0.134 × 0.02
Theta range for data collection	3.699° to 73.612°	3.571° to 73.737°
Limiting indices	$-12 \le h \le 16$, $-16 \le k \le 14$, $-21 \le l \le 21$	$-12 \le h \le 10$, $-16 \le k \le 12$, $-19 \le l \le 18$
Reflections collected	18550	14309
Independent reflections	10581 [R_{int} = 0.0364, R_{sigma} = 0.0401]	8107 [R_{int} = 0.0362, R_{sigma} = 0.0488]
Data / restraints / parameters	10581/25/599	8107/0/605
Goodness-of-fit on F^2	1.050	1.043
Final *R* indices [$I>2\sigma(I)$]	R_1 = 0.0675, wR_2 = 0.1941	R_1 = 0.0498, wR_2 = 0.1308
R indices (all data)	R_1 = 0.0760, wR_2 = 0.2039	R_1 = 0.0603, wR_2 = 0.1400
Largest diff. peak and hole	0.762/-0.929 e.Å^{-3}	1.184/-0.630 e.Å^{-3}

Table S18 Selected bond distances (Å), bond angles (°) in $[Cr(phen)_2(bipy)](CF_3SO_3)_3$ (**9**).

Bond distances (Å)			
Cr(1)-N(1)	2.054(3)	Cr(1)-N(4)	2.053(2)
Cr(1)-N(2)	2.050(3)	Cr(1)-N(5)	2.048(2)
Cr(1)-N(3)	2.057(2)	Cr(1)-N(6)	2.041(3)
Bond angles (°)			
N(1)-Cr(1)-N(3)	95.19(10)	N(5)-Cr(1)-N(3)	173.05(10)
N(2)-Cr(1)-N(1)	81.18(11)	N(5)-Cr(1)-N(4)	94.09(10)
N(2)-Cr(1)-N(3)	91.48(10)	N(6)-Cr(1)-N(1)	92.95(11)
N(2)-Cr(1)-N(4)	94.09(10)	N(6)-Cr(1)-N(2)	171.40(10)
N(4)-Cr(1)-N(1)	173.63(10)	N(6)-Cr(1)-N(3)	95.33(10)
N(4)-Cr(1)-N(3)	80.61(10)	N(6)-Cr(1)-N(4)	92.22(10)
N(5)-Cr(1)-N(1)	90.46(10)	N(6)-Cr(1)-N(5)	80.31(10)
N(5)-Cr(1)-N(2)	93.39(11)		

Table S19 Selected bond distances (Å), bond angles (°) in $[Cr(phen)_2(dpma)](CF_3SO_3)_3$ (**10**).

Bond distances (Å)			
Cr(1)-N(1)	2.046(2)	Cr(1)-N(4)	2.063(2)
Cr(1)-N(2)	2.044(3)	Cr(1)-N(5)	2.061(2)
Cr(1)-N(3)	2.064(2)	Cr(1)-N(6)	2.078(2)
Bond angles (°)			
N(1)-Cr(1)-N(3)	98.68(10)	N(2)-Cr(1)-N(6)	87.65(10)
N(1)-Cr(1)-N(4)	90.42(9)	N(3)-Cr(1)-N(6)	89.11(9)
N(1)-Cr(1)-N(5)	92.09(9)	N(4)-Cr(1)-N(3)	80.11(10)
N(1)-Cr(1)-N(6)	169.21(9)	N(4)-Cr(1)-N(6)	98.30(9)
N(2)-Cr(1)-N(1)	85.41(10)	N(5)-Cr(1)-N(3)	94.00(9)
N(2)-Cr(1)-N(3)	172.78(10)	N(5)-Cr(1)-N(4)	173.89(10)
N(2)-Cr(1)-N(4)	93.96(10)	N(5)-Cr(1)-N(6)	79.86(9)
N(2)-Cr(1)-N(5)	91.79(10)		

Table S20 Interplanar angles (°) in $[Cr(phen)_2(bipy)](CF_3SO_3)_3$ (**9**).

Phen1 N1 C1 C2 C3 C4 C5 C6 C7 C8 C9 C10 C11 C12 N2

Phen2 N3 C13 C14 C15 C16 C17 C18 C19 C29 C21 C22 C23 C24 N4

Bipy1 N5 C25 C26 C27 C28 C29 C39 C31 C32 C33 C34 N6

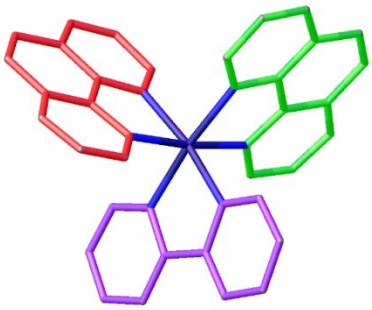

	Phen2	Bipy1
Phen1	93.3°	87.3°
Phen2		91.9°

The error is typically ±0.1°.

Table S21 Interplanar angles (°) in $[Cr(phen)_2(dpma)](CF_3SO_3)_3$ (**10**).

Phen1 N3 C19 C20 C21 C22 C23 C24 C25 C26 C27 C28 C29 C30 N4

Phen2 N5 C31 C32 C33 C34 C35 C36 C37 C38 C39 C40 C41 C42 N6

Pyr1 N1 C7 C8 C9 C10 C11

Pyr2 N2 C14 C15 C16 C17 C18

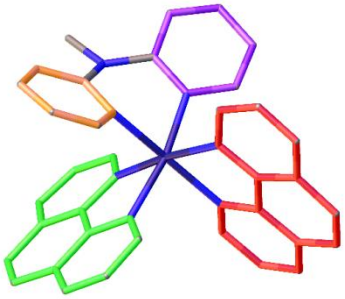

	Phen2	Pyr1	Pyr2
Phen1	90.2°	94.4°	55.9°
Phen2		53.7°	56.3°
Pyr1			38.9°

The error is typically ±0.1°.

Table S22. Cr-N bond length ($d_{Cr\text{-}N}$) and bite N-Cr-N angle, measured and calculated from crystallographic structures.

Complex	$d_{Cr\text{-}N}$[a] (Å)		Chelate N-Cr-N angle[b] (°)	
	phen	N-N'	phen	N-N'
$[Cr(phen)_3](PF_6)_3$ (**2**)	2.051(4)		81.0(1)	
$[Cr(phen)_2(phenBr)](PF_6)_3$ (**3**)	2.057(4)	2.051(4)	80.5(1)	80.8(1)
$[Cr(phen)_2(phenAlkyn)](BF_4)_3$ (**6**)	2.051(4)	2.063(4)	81.1(1)	80.4(1)
$[Cr(phen)_2(phenNO_2)](CF_3SO_3)_3$ (**7**)	2.050(4)	2.050(4)	81.1(1)	80.9(1)
$[Cr(phen)_2(phenNH_2)](CF_3SO_3)_3$ (**8**)	2.051(4)	2.058(4)	80.8(1)	81.1(1)
$[Cr(phen)_2(bipy)](CF_3SO_3)_3$ (**9**)	2.054(4)	2.045(4)	80.9(1)	80.3(1)
$[Cr(phen)_2(dpma)](CF_3SO_3)_3$ (**10**)	2.067(4)	2.045(4)	80.0(1)	85.4(1)

[a] Average Cr-N bond lengths. [b] Average N-Cr-N bite angles.

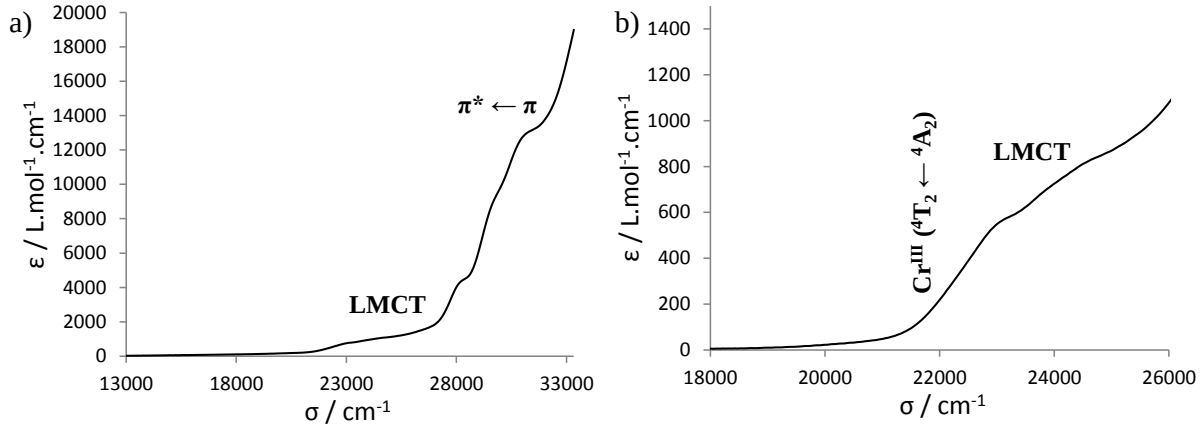

Fig. S11 Absorption spectrum of $[Cr(phen)_3](PF_6)_3$ (**2**) in acetonitrile at room temperature, $C = 2.00\times10^{-4}$ mol.L^{-1} : a) 1 mm optical path, b) 1 cm optical path (zoom).

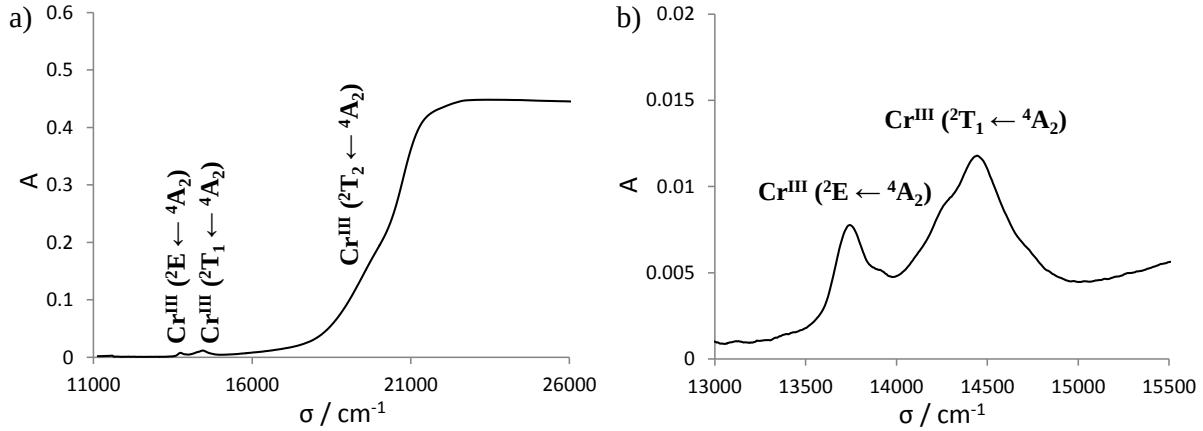

Fig. S12 Absorption spectrum of $[Cr(phen)_3](PF_6)_3$ (**2**) in the solid state at room temperature : a) full spectrum, b) zoom on the spin-flip transitions at low energy.

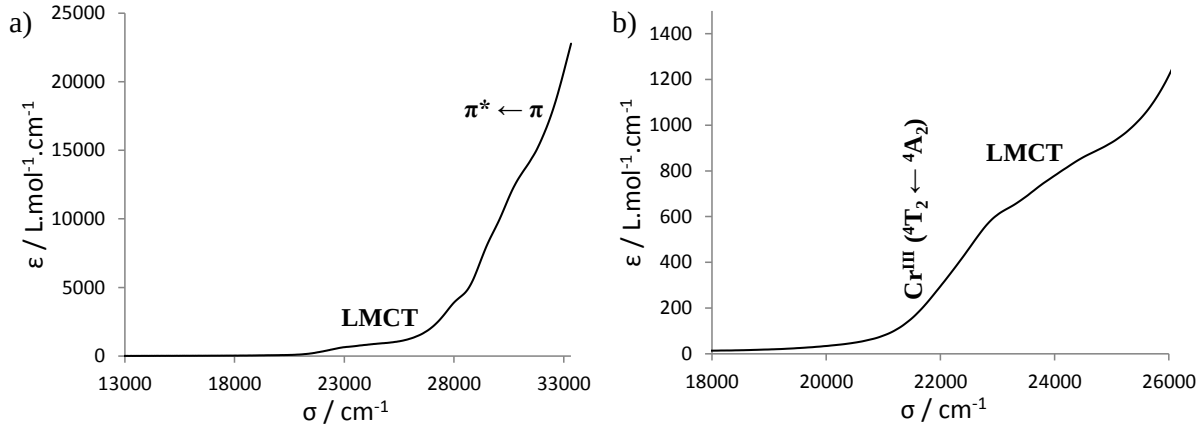

Fig. S13 Absorption spectrum of $[Cr(phen)_2(phenBr)](PF_6)_3$ (**3**) in acetonitrile at room temperature, $C = 2.15\times10^{-4}$ mol.L^{-1} : a) 1 mm optical path, b) 1 cm optical path (zoom).

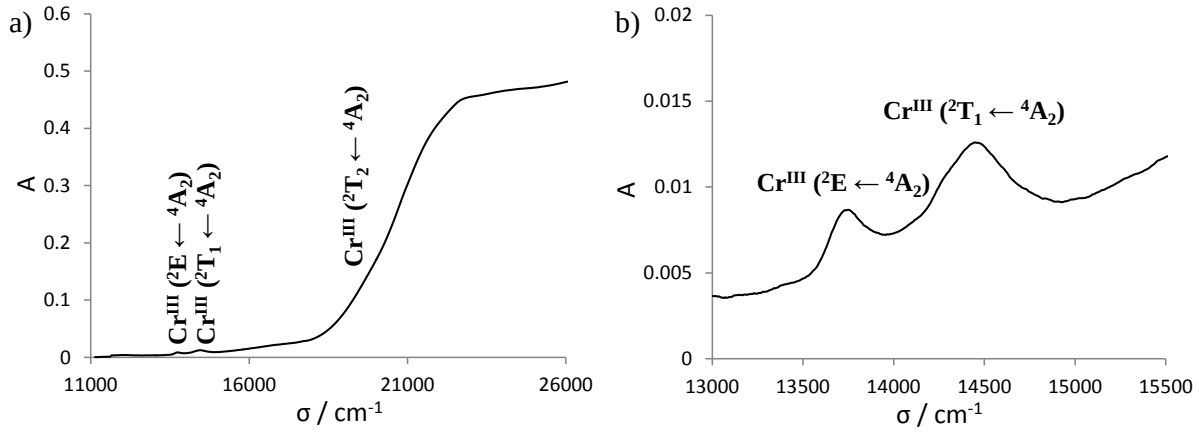

Fig. S14 Absorption spectrum of $[Cr(phen)_2(phenBr)](PF_6)_3$ (**3**) in the solid state at room temperature : a) full spectrum, b) zoom on the spin-flip transitions at low energy.

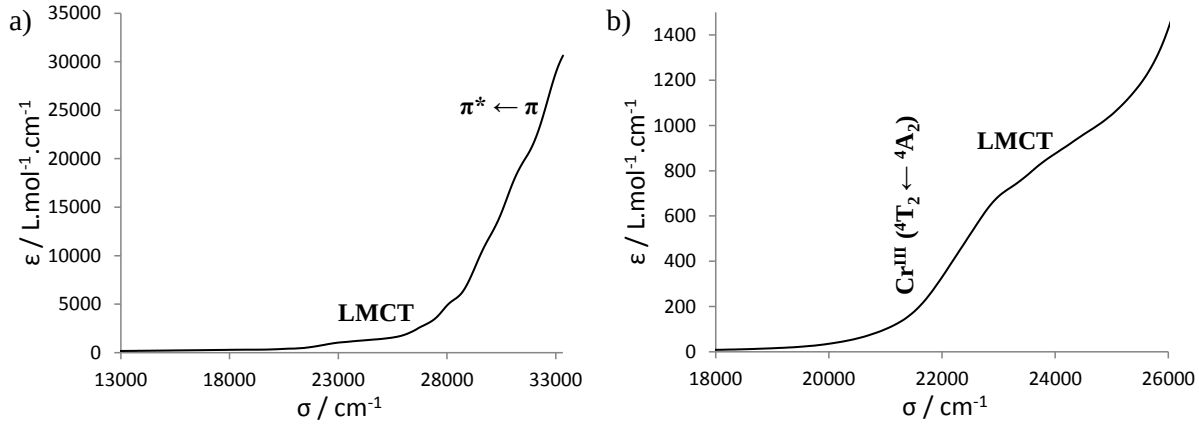

Fig. S15 Absorption spectrum of $[Cr(phen)_2(phenAlkyn)](BF_4)_3$ (**6**) in acetonitrile at room temperature, $C = 2.05\times10^{-4}$ mol.L^{-1} : a) 1 mm optical path, b) 1 cm optical path (zoom).

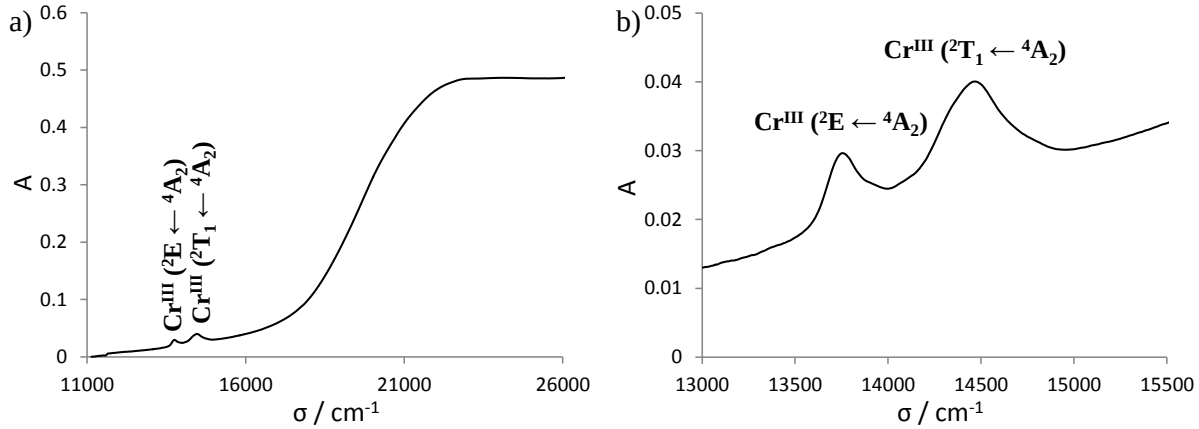

Fig. S16 Absorption spectrum of $[Cr(phen)_2(phenAlkyn)](BF_4)_3$ (**6**) in the solid state at room temperature : a) full spectrum, b) zoom on the spin-flip transitions at low energy.

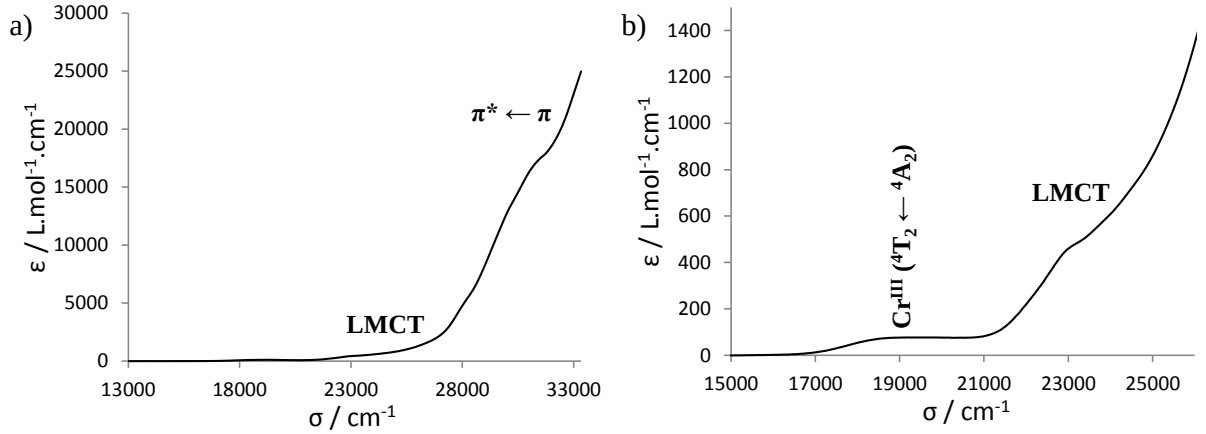

Fig. S17 Absorption spectrum of $[Cr(phen)_2(phenNO_2)](CF_3SO_3)_3$ (**7**) in acetonitrile at room temperature, $C = 2.09\times10^{-4}$ mol.L^{-1} : a) 1 mm optical path, b) 1 cm optical path (zoom).

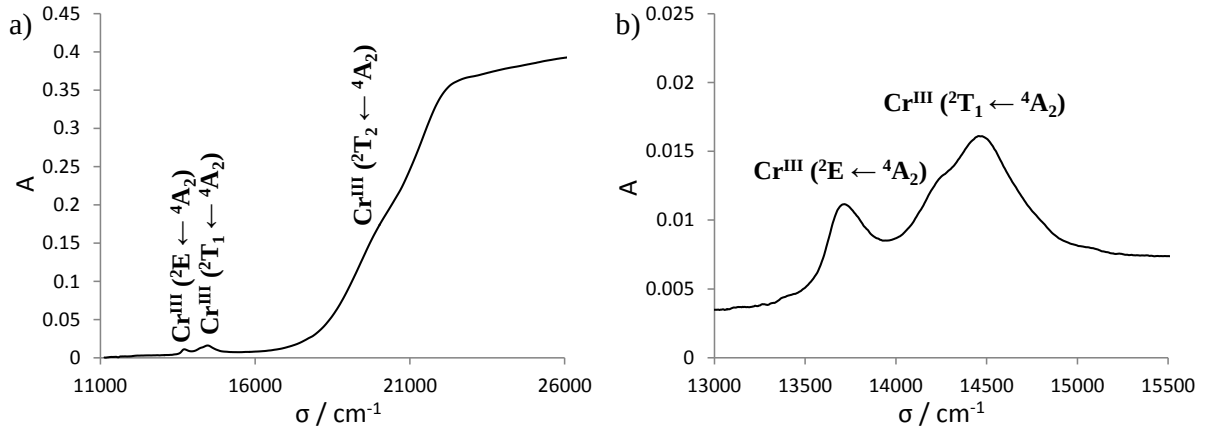

Fig. S18 Absorption spectrum of $[Cr(phen)_2(phenNO_2)](CF_3SO_3)_3$ (**7**) in the solid state at room temperature : a) full spectrum, b) zoom on the spin-flip transitions at low energy.

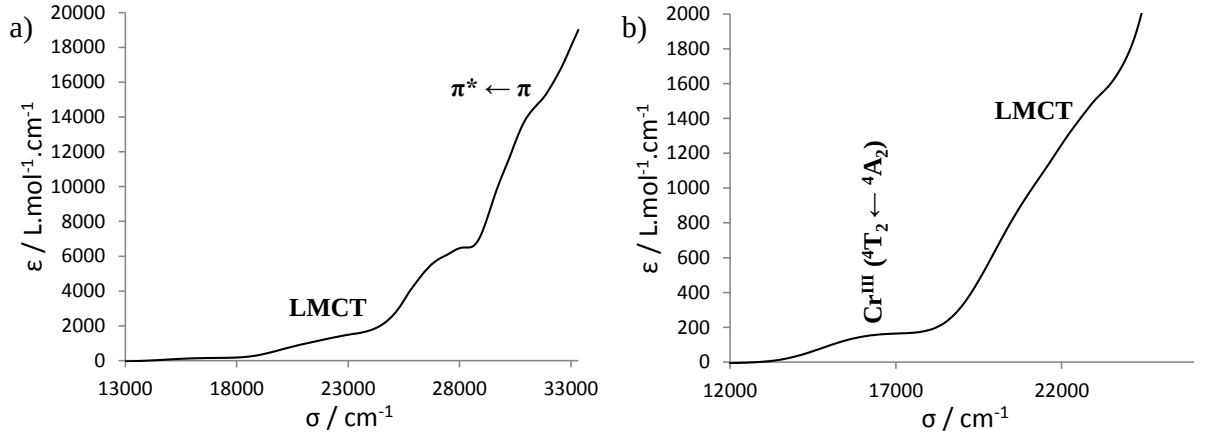

Fig. S19 Absorption spectrum of $[Cr(phen)_2(phenNH_2)](CF_3SO_3)_3$ (**8**) in acetonitrile at room temperature, $C = 1.97\times10^{-4}$ mol.L^{-1} : a) 1 mm optical path, b) 1 cm optical path (zoom).

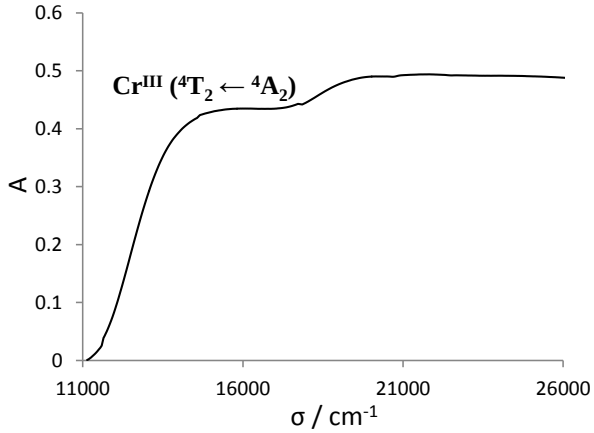

Fig. S20 Absorption spectrum of $[Cr(phen)_2(phenNH_2)](CF_3SO_3)_3$ (**8**) in the solid state at room temperature.

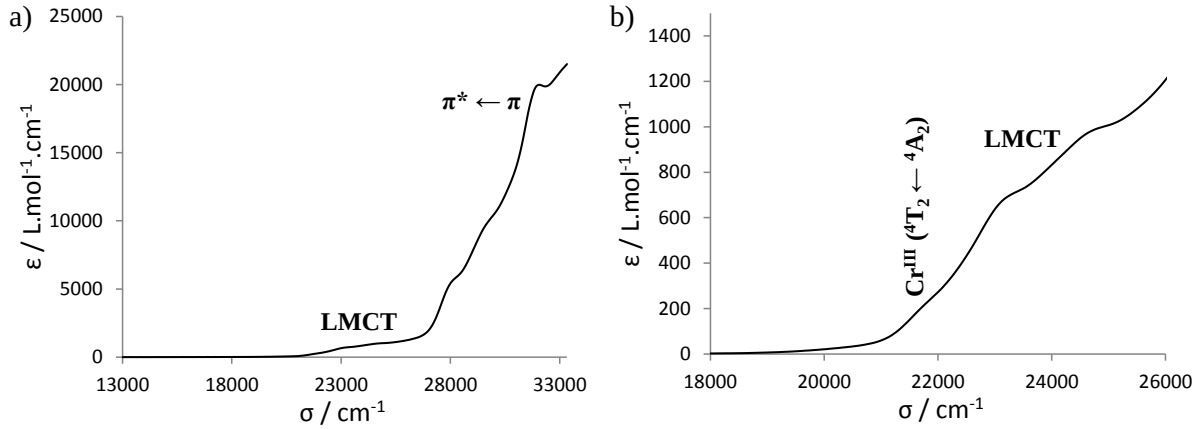

Fig. S21 Absorption spectrum of $[Cr(phen)_2(bipy)](BF_4)_3$ (**9**) in acetonitrile at room temperature, $C = 2.47\times10^{-4}$ mol.L^{-1} : a) 1 mm optical path, b) 1 cm optical path (zoom).

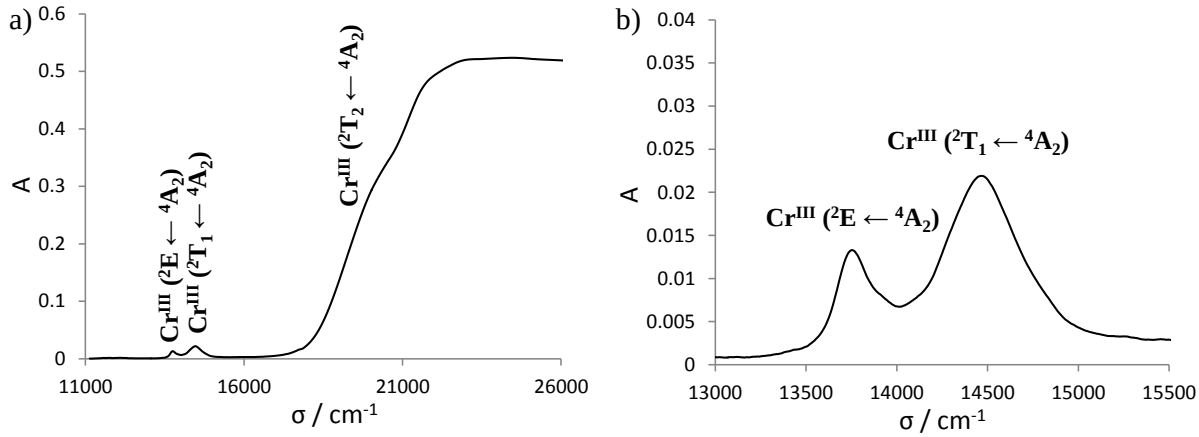

Fig. S22 Absorption spectrum of $[Cr(phen)_2(bipy)](BF_4)_3$ (**9**) in the solid state at room temperature : a) full spectrum, b) zoom on the spin-flip transitions at low energy.

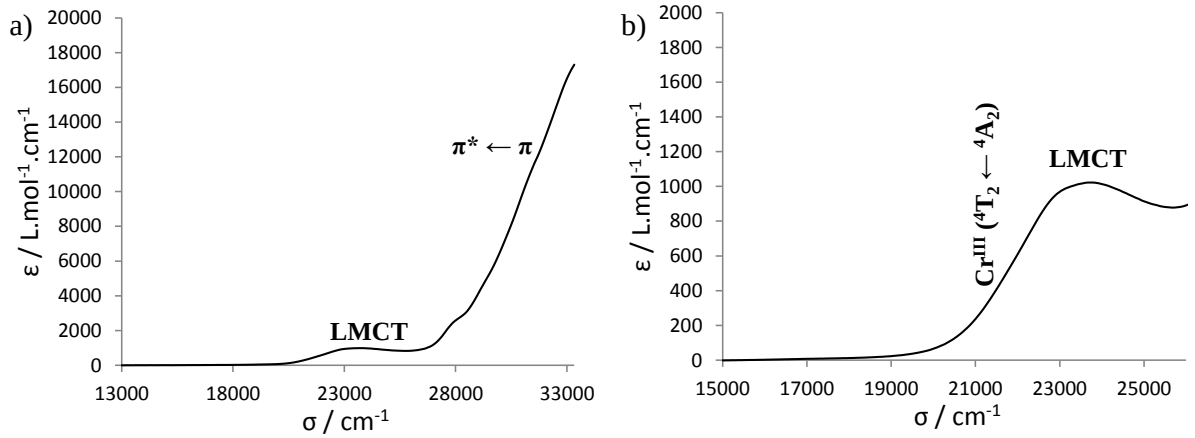

Fig. S23 Absorption spectrum of $[Cr(phen)_2(dpma)](CF_3SO_3)_3$ (**10**) in acetonitrile at room temperature, $C = 2.08\times10^{-4}$ mol.L^{-1} : a) 1 mm optical path, b) 1 cm optical path (zoom).

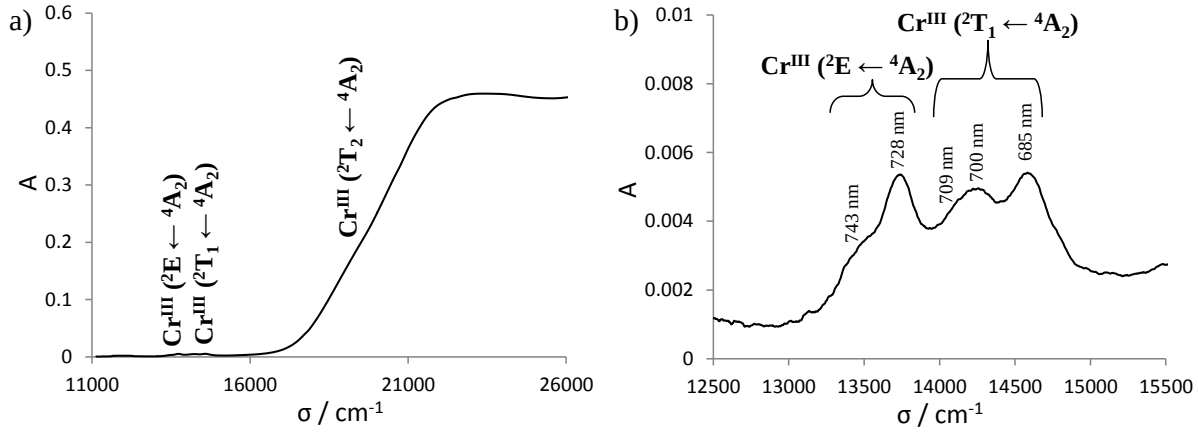

Fig. S24 Absorption spectrum of $[Cr(phen)_2(dpma)](CF_3SO_3)_3$ (**10**) in the solid state at room temperature : a) full spectrum, b) zoom on the spin-flip transitions at low energy.

Table S23 Electronic absorption spectra of heteroleptic Cr(III)N_6 ter-bidentate complexes recorded in acetonitrile or in the solid state at 298 K.

Compound	Solvent	λ / nm	$\bar{\upsilon}$ / cm^{-1}	ε / $M^{-1}.cm^{-1}$	Assignment
$[Cr(phen)_3](PF_6)_3$ (**2**)	CH_3CN	320	31250	13000	$^4[^1(\pi^*\leftarrow\pi)]$
		337	29674	8990	
		355	28139	4310	LMCT
		406	24630	828	LMCT / $^4[^3(\pi^*\leftarrow\pi)]$
		431	23202	579	
		453	22075	243	Cr ($^4T_2 \leftarrow {}^4A_2$)
		692[a]	14451		Cr ($^2T_1 \leftarrow {}^4A_2$)
		700[sh,a]	14286		
		728[a]	13736		Cr ($^2E \leftarrow {}^4A_2$)
$[Cr(phen)_2(phenBr)](PF_6)_3$ (**3**)	CH_3CN	323	30960	13000	$^4[^1(\pi^*\leftarrow\pi)]$
		338	29586	8380	
		355	28169	4040	LMCT
		408	24510	851	LMCT / $^4[^3(\pi^*\leftarrow\pi)]$
		434	23041	616	
		452	22124	335	Cr ($^4T_2 \leftarrow {}^4A_2$)
		692[a]	14451		Cr ($^2T_1 \leftarrow {}^4A_2$)
		700[sh,a]	14286		
		728[a]	13736		Cr ($^2E \leftarrow {}^4A_2$)
$[Cr(phen)_2(phenAlkyn)](BF_4)_3$ (**6**)	CH_3CN	317	31546	19800	$^4[^1(\pi^*\leftarrow\pi)]$
		334	29940	11900	
		355	28169	5220	LMCT
		373	26810	2690	
		406	24631	981	LMCT / $^4[^3(\pi^*\leftarrow\pi)]$
		418	23923	863	
		431	23202	724	
		448	22321	452	Cr ($^4T_2 \leftarrow {}^4A_2$)
		691[a]	14472		Cr ($^2T_1 \leftarrow {}^4A_2$)
		699[sh,a]	14306		
		728[a]	13717		Cr ($^2E \leftarrow {}^4A_2$)

$[Cr(phen)_2(phenNO_2)](CF_3SO_3)_3$ (**7**)	CH_3CN	317	31546	17600	$^4[^1(\pi^*\leftarrow\pi)]$
		331	30211	13500	
		355	28169	5260	LMCT
		409	24450	708	LMCT / $^4[^3(\pi^*\leftarrow\pi)]$
		419	23866	585	
		431	23202	483	Cr ($^4T_2 \leftarrow {}^4A_2$)
		520	19231	77	Cr ($^2T_1 \leftarrow {}^4A_2$)
		691[a]	14472		
		702[sh,a]	14245		Cr ($^2E \leftarrow {}^4A_2$)
		729[a]	13717		
$[Cr(phen)_2(phenNH_2)](CF_3SO_3)_3$ (**8**)	CH_3CN	316	31646	15200	$^4[^1(\pi^*\leftarrow\pi)]$
		334	29940	10900	
		355	28169	6600	LMCT
		366	27322	6090	
		436	22936	1490	LMCT / $^4[^3(\pi^*\leftarrow\pi)]$
		471	21231	1030	
		600	16670	161	Cr ($^4T_2 \leftarrow {}^4A_2$)
$[Cr(phen)_2(bipy)](BF_4)_3$ (**9**)	CH_3CN	314	31847	19600	$^4[^1(\pi^*\leftarrow\pi)]$
		336	29762	10000	
		356	28090	5600	LMCT
		401	24938	1000	LMCT / $^4[^3(\pi^*\leftarrow\pi)]$
		427	23419	718	
		456	21930	256	Cr ($^4T_2 \leftarrow {}^4A_2$)
		691[a]	14472		Cr ($^2T_1 \leftarrow {}^4A_2$)
		728[a]	13717		Cr ($^2E \leftarrow {}^4A_2$)
$[Cr(phen)_2(dpma)](CF_3SO_3)_3$ (**10**)	CH_3CN	316	31646	11900	$^4[^1(\pi^*\leftarrow\pi)]$
		340	29412	5020	
		355	28169	2740	LMCT
		423	23641	1020	LMCT / $^4[^3(\pi^*\leftarrow\pi)]$
		460	21739	502	Cr ($^4T_2 \leftarrow {}^4A_2$)
		685[a]	14599		Cr ($^2T_1 \leftarrow {}^4A_2$)
		700[a]	14286		
		709[sh,a]	14104		
		728[a]	13736		Cr ($^2E \leftarrow {}^4A_2$)
		743[sh,a]	13459		

Energies are given for the maximum of the band envelope in cm^{-1}. [a] Transitions observed in the solid state. [sh] Shoulder observed in the solid state

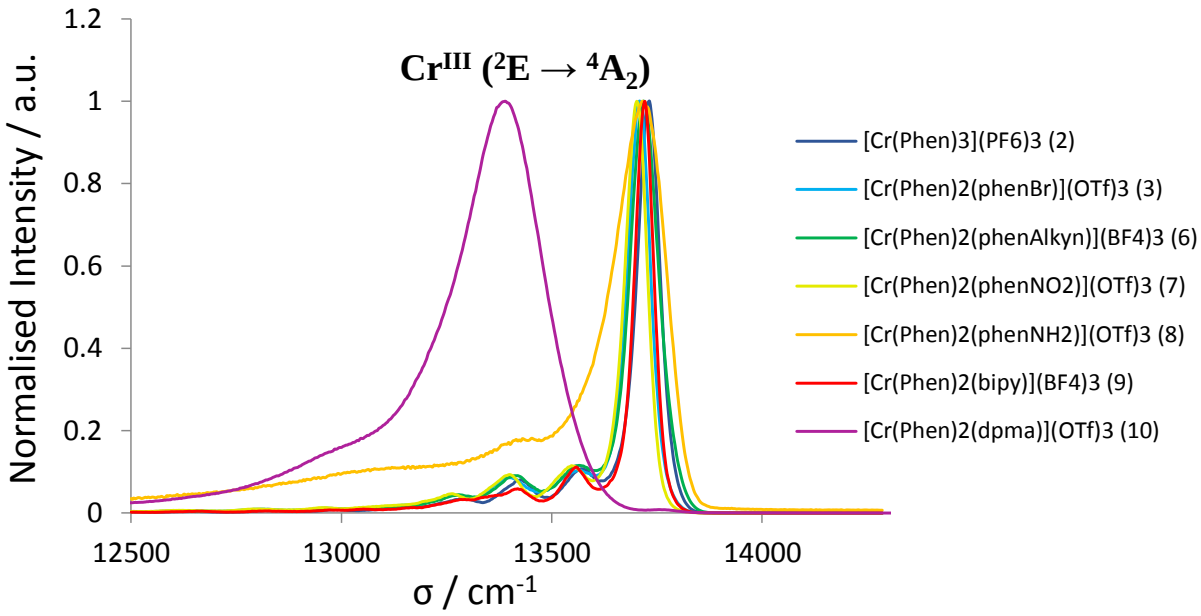

Fig. S25 Normalized emission spectrum at 10 K in frozen solution acetonitrile/propionitrile (6/4), λ_{exc} = 355 nm ($\bar{\upsilon}_{exc}$ = 28170 cm^{-1}), integration time = 0.3 s, cutoff filter 650 nm, of $[Cr(phen)_3](PF_6)_3$ (**2**) (blue, slit(em) = slit(exc) = 0.8 nm), $[Cr(phen)_2(phenBr)](PF_6)_3$ (**3**) (light blue, slit(em) = slit(exc) = 0.7 nm), $[Cr(phen)_2(phenAlkyn)](BF_4)_3$ (**6**) (green, slit(em) = slit(exc) = 2.0 nm), $[Cr(phen)_2(phenNO_2)](CF_3SO_3)_3$ (**7**) (yellow, slit(em) = slit(exc) = 0.8 nm, solvent : acetonitrile), $[Cr(phen)_2(phenNH_2)](CF_3SO_3)_3$ (**8**) (orange, slit(em) = slit(exc) = 3.0 nm), $[Cr(phen)_2(bipy)](BF_4)_3$ (**9**) (red, slit(em) = slit(exc) = 0.7 nm), $[Cr(phen)_2(dpma)](CF_3SO_3)_3$ (**10**) (purple, slit(em) = slit(exc) = 1.3 nm).

Table S24 Emission spectra of heteroleptic Cr(III)N_6 ter-bidentate complexes recorded at 10 K in frozen acetonitrile/propionitrile mixture (6/4).

Compound	$\lambda_{excitation}$ / nm	$\lambda_{emission}$ / nm	$\bar{\upsilon}_{emission}$ / cm^{-1}	Assignment
$[Cr(phen)_3](PF_6)_3$ (**2**)	355	728.2	13732	Cr ($^2E(v=0) \rightarrow {}^4A_2(v=0)$)
		736.8	13572	Cr ($^2E(v=0) \rightarrow {}^4A_2(v=1)$)
		745.0	13423	Cr ($^2E(v=0) \rightarrow {}^4A_2(v=2)$)
		752.4	13290	Cr ($^2E(v=0) \rightarrow {}^4A_2(v=3)$)
$[Cr(phen)_2(phenBr)](PF_6)_3$ (**3**)	355	729.5	13708	Cr ($^2E(v=0) \rightarrow {}^4A_2(v=0)$)
		737.8	13554	Cr ($^2E(v=0) \rightarrow {}^4A_2(v=1)$)
		746.0	13405	Cr ($^2E(v=0) \rightarrow {}^4A_2(v=2)$)
		753.4	13273	Cr ($^2E(v=0) \rightarrow {}^4A_2(v=3)$)
$[Cr(phen)_2(phenAlkyn)](BF_4)_3$ (**6**)	355	728.8	13721	Cr ($^2E(v=0) \rightarrow {}^4A_2(v=0)$)
		737.2	13565	Cr ($^2E(v=0) \rightarrow {}^4A_2(v=1)$)
		745.4	13416	Cr ($^2E(v=0) \rightarrow {}^4A_2(v=2)$)
		753.4	13273	Cr ($^2E(v=0) \rightarrow {}^4A_2(v=3)$)
$[Cr(phen)_2(phenNO_2)](CF_3SO_3)_3$ (**7**)	355	729.8	13702	Cr ($^2E(v=0) \rightarrow {}^4A_2(v=0)$)
		738.2	13546	Cr ($^2E(v=0) \rightarrow {}^4A_2(v=1)$)
		746.4	13398	Cr ($^2E(v=0) \rightarrow {}^4A_2(v=2)$)
		754.0	13263	Cr ($^2E(v=0) \rightarrow {}^4A_2(v=3)$)
$[Cr(phen)_2(phenNH_2)](CF_3SO_3)_3$ (**8**)	355	729	13717	Cr ($^2E \rightarrow {}^4A_2$)
$[Cr(phen)_2(bipy)](BF_4)_3$ (**9**)	355	728.8	13721	Cr ($^2E(v=0) \rightarrow {}^4A_2(v=0)$)
		737.6	13557	Cr ($^2E(v=0) \rightarrow {}^4A_2(v=1)$)
		745.4	13416	Cr ($^2E(v=0) \rightarrow {}^4A_2(v=2)$)
		752.4	13291	Cr ($^2E(v=0) \rightarrow {}^4A_2(v=3)$)
$[Cr(phen)_2(dpma)](CF_3SO_3)_3$ (**10**)	355	727 ^{sh}	13755	Cr ($^2E \rightarrow {}^4A_2$)
		747	13387	

Energies are given for the maximum of the band envelope in cm^{-1}. ^{sh} Shoulder.

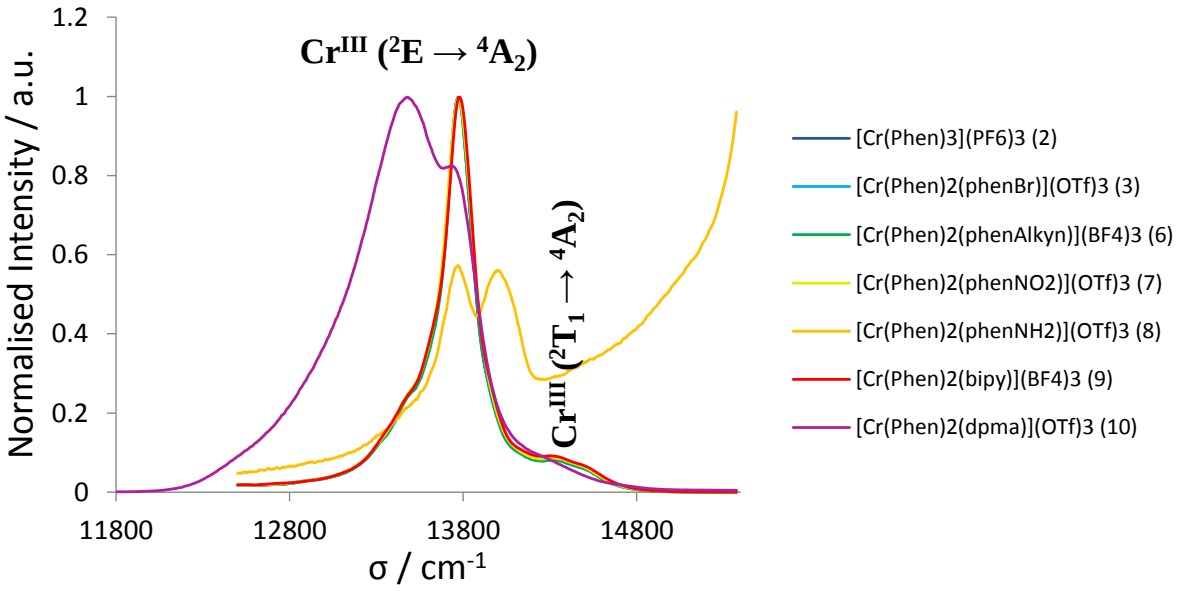

Fig. S26 Normalized emission spectrum at 293 K in degassed acetonitrile, λ_{exc} = 355 nm ($\bar{\upsilon}_{exc}$ = 28170 cm^{-1}), integration time = 0.3 s, of $[Cr(phen)_3](PF_6)_3$ (**2**) (blue, slit(em) = slit(exc) = 3.0 nm), $[Cr(phen)_2(phenBr)](PF_6)_3$ (**3**) (light blue, slit(em) = slit(exc) = 2.0 nm), $[Cr(phen)_2(phenAlkyn)](BF_4)_3$ (**6**) (green, slit(em) = slit(exc) = 2.0 nm), $[Cr(phen)_2(phenNO_2)](CF_3SO_3)_3$ (**7**) (yellow, slit(em) = slit(exc) = 3.0 nm), $[Cr(phen)_2(phenNH_2)](CF_3SO_3)_3$ (**8**) (orange, slit(em) = slit(exc) = 5.0 nm), $[Cr(phen)_2(bipy)](BF_4)_3$ (**9**) (red, slit(em) = slit(exc) = 3.0 nm), $[Cr(phen)_2(dpma)](CF_3SO_3)_3$ (**10**) (purple, slit(em) = slit(exc) = 5.0 nm).

Table S25 Emission spectra of heteroleptic Cr(III)N_6 ter-bidentate complexes recorded at 293 K in degassed acetonitrile.

Compound	$\lambda_{excitation}$ / nm	$\lambda_{emission}$ / nm	$\bar{\upsilon}_{emission}$ / cm^{-1}	Assignment
$[Cr(phen)_3](PF_6)_3$ (**2**)	355	689 ^{sh} 698 726	14514 14327 13774	Cr ($^2T_1 \rightarrow {}^4A_2$) Cr ($^2E \rightarrow {}^4A_2$)
$[Cr(phen)_2(phenBr)](PF_6)_3$ (**3**)	355	689 ^{sh} 698 726	14514 14327 13774	Cr ($^2T_1 \rightarrow {}^4A_2$) Cr ($^2E \rightarrow {}^4A_2$)
$[Cr(phen)_2(phenAlkyn)](BF_4)_3$ (**6**)	355	690 ^{sh} 698 726	14493 14327 13774	Cr ($^2T_1 \rightarrow {}^4A_2$) Cr ($^2E \rightarrow {}^4A_2$)
$[Cr(phen)_2(phenNO_2)](CF_3SO_3)_3$ (**7**)	355	689 ^{sh} 698 726	14514 14327 13774	Cr ($^2T_1 \rightarrow {}^4A_2$) Cr ($^2E \rightarrow {}^4A_2$)
$[Cr(phen)_2(phenNH_2)](CF_3SO_3)_3$ (**8**)	355	726	13774	Cr ($^2E \rightarrow {}^4A_2$)
$[Cr(phen)_2(bipy)](BF_4)_3$ (**9**)	355	688 ^{sh} 699 726	14535 14306 13774	Cr ($^2T_1 \rightarrow {}^4A_2$) Cr ($^2E \rightarrow {}^4A_2$)
$[Cr(phen)_2(dpma)](CF_3SO_3)_3$ (**10**)	355	700 ^{sh} 728 742	14286 13736 13477	Cr ($^2T_1 \rightarrow {}^4A_2$) Cr ($^2E \rightarrow {}^4A_2$)

Energies are given for the maximum of the band envelope in cm^{-1}. ^{sh} Shoulder.

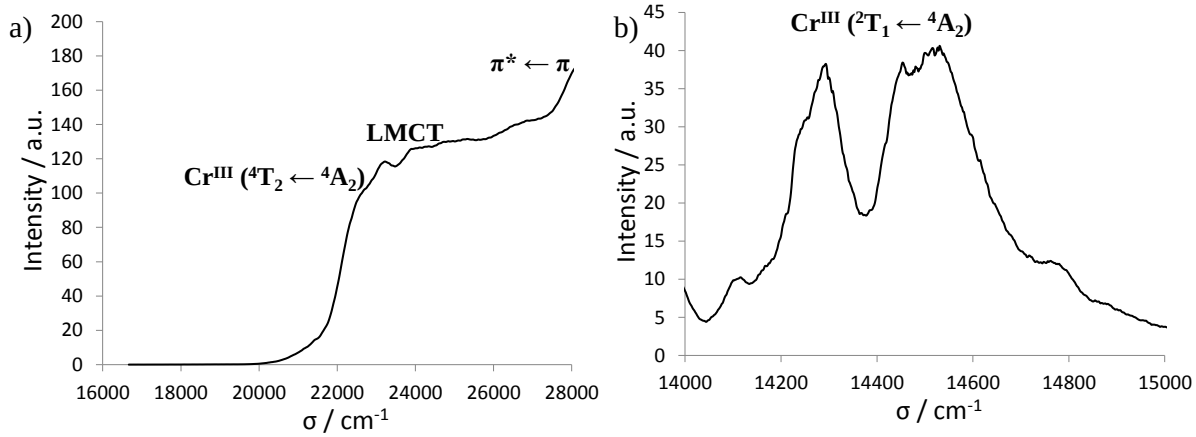

Fig. S27 Excitation spectrum of $[Cr(phen)_3](PF_6)_3$ (**2**) at 10 K : a) in frozen solution acetonitrile/propionitrile (6/4), λ_{em} = 730 nm, slit(em) = slit(exc) = 1.2 nm, integration time = 0.3 s, cutoff filter 715 nm, b) in solid state, λ_{em} = 729 nm, slit(em) = slit(exc) = 1.0 nm, integration time = 0.3 s, cutoff filter 715 nm.

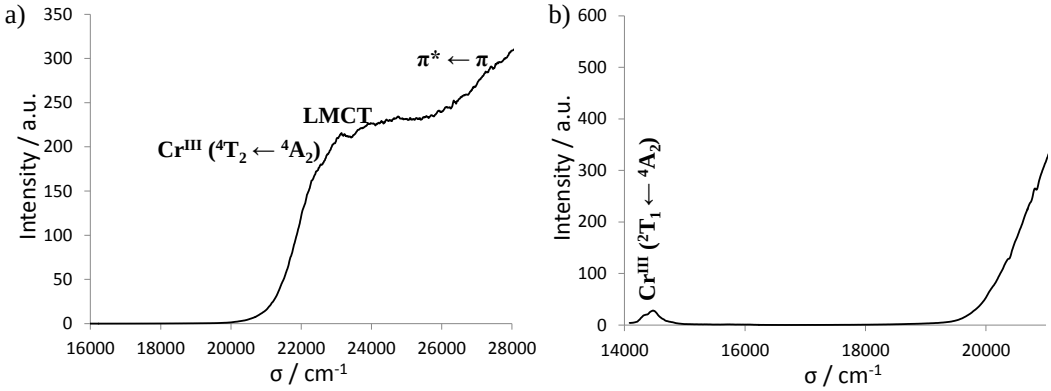

Fig. S28 Excitation spectrum of $[Cr(phen)_2(phenBr)](PF_6)_3$ (**3**) at 10 K : a) in frozen solution acetonitrile/propionitrile (6/4), λ_{em} = 729 nm, slit(em) = slit(exc) = 0.7 nm, integration time = 0.5 s, cutoff filter 715 nm, b) in solid state, λ_{em} = 732 nm, slit(em) = slit(exc) = 0.5 nm, integration time = 0.3 s, cutoff filter 715 nm.

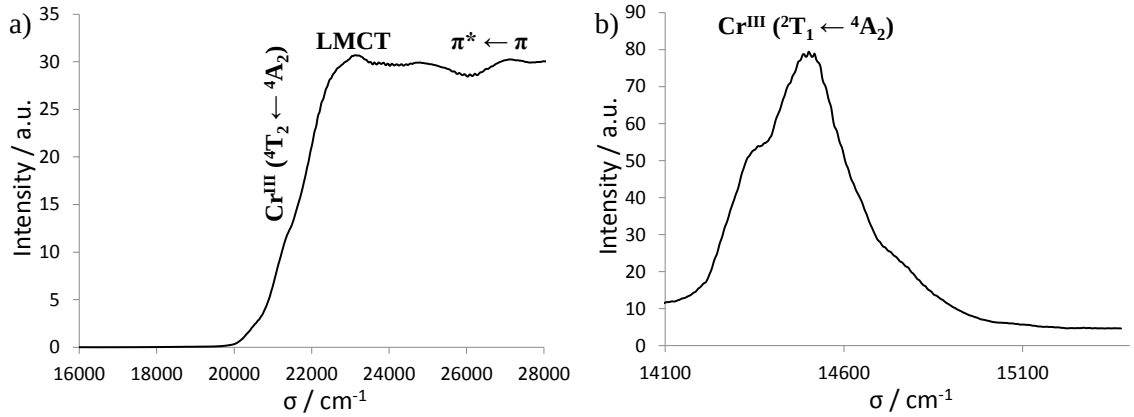

Fig. S29 Excitation spectrum of $[Cr(phen)_2(phenAlkyn)](BF_4)_3$ (**6**) at 10 K : a) in frozen solution acetonitrile/propionitrile (6/4), λ_{em} = 729 nm, slit(em) = slit(exc) = 1.9 nm, integration time = 0.3 s, cutoff filter 715 nm, b) in solid state, λ_{em} = 731 nm, slit(em) = slit(exc) = 1.4 nm, integration time = 0.3 s, cutoff filter 715 nm.

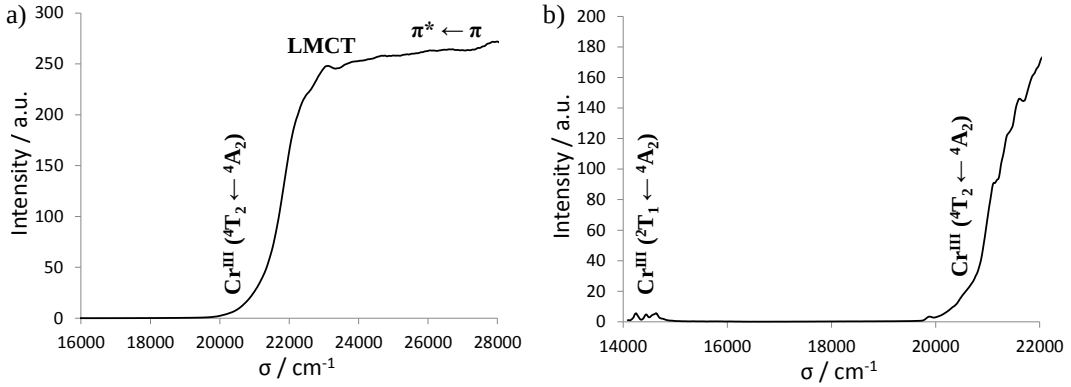

Fig. S30 Excitation spectrum of $[Cr(phen)_2(phenNO_2)](CF_3SO_3)_3$ (**7**) at 10 K : a) in frozen solution acetonitrile, λ_{em} = 730 nm, slit(em) = slit(exc) = 0.8 nm, integration time = 0.3 s, cutoff filter 715 nm, b) in solid state, λ_{em} = 728 nm, slit(em) = slit(exc) = 0.7 nm, integration time = 0.3 s, cutoff filter 715 nm.

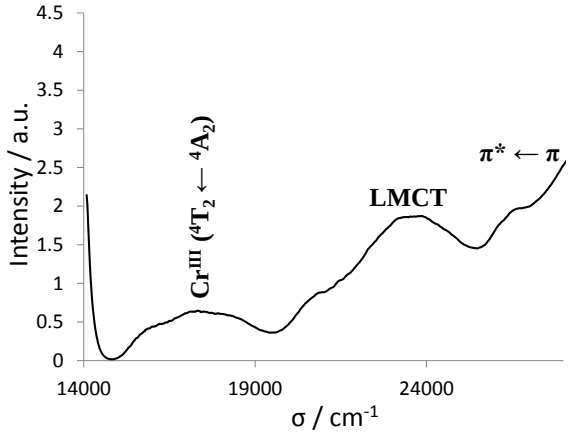

Fig. S31 Excitation spectrum of $[Cr(phen)_2(phenNH_2)](CF_3SO_3)_3$ (**8**) at 10 K in frozen solution acetonitrile/propionitrile (6/4), λ_{em} = 729 nm, slit(em) = slit(exc) = 3.0 nm, integration time = 0.3 s, cutoff filter 715 nm.

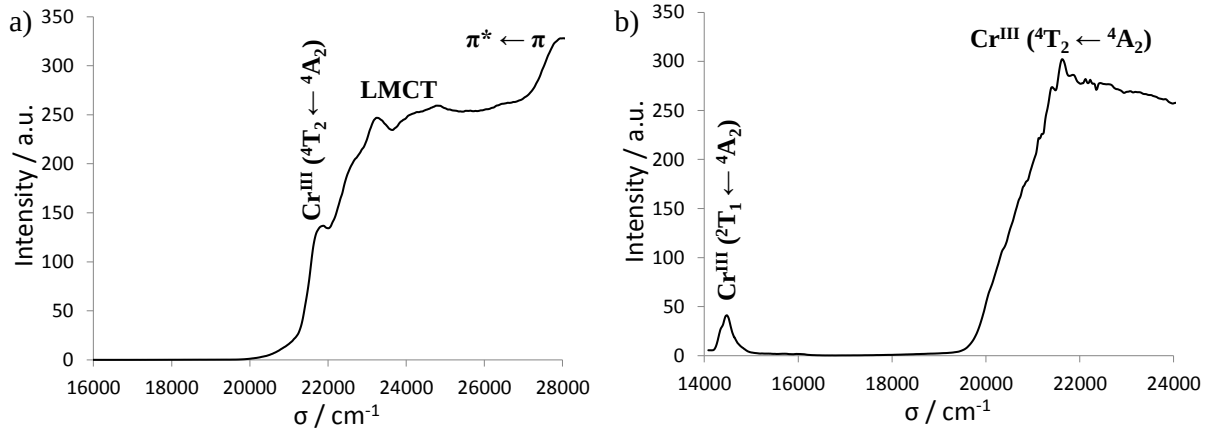

Fig. S32 Excitation spectrum of $[Cr(phen)_2(bipy)](BF_4)_3$ (**9**) at 10 K : a) in frozen solution acetonitrile/propionitrile (6/4), λ_{em} = 729 nm, slit(em) = slit(exc) = 0.8 nm, integration time = 0.3 s, cutoff filter 715 nm, b) in solid state, λ_{em} = 732 nm, slit(em) = slit(exc) = 0.7 nm, integration time = 0.3 s, cutoff filter 715 nm.

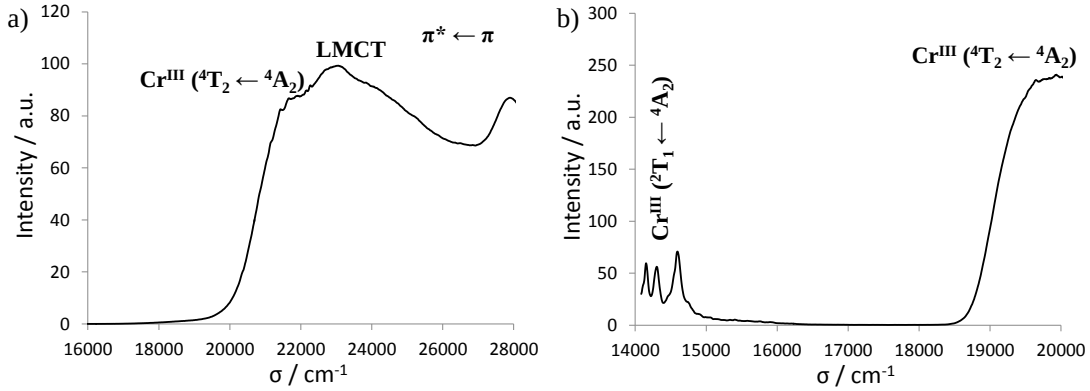

Fig. S33 Excitation spectrum of $[Cr(phen)_2(dpma)](CF_3SO_3)_3$ (**10**) at 10 K : a) in frozen solution acetonitrile/propionitrile (6/4), λ_{em} = 747 nm, slit(em) = slit(exc) = 1.2 nm, integration time = 0.3 s, cutoff filter 715 nm, b) in solid state, λ_{em} = 743 nm, slit(em) = slit(exc) = 0.8 nm, integration time = 0.2 s, cutoff filter 715 nm.

Table S26 Excitation spectra of heteroleptic Cr(III)N_6 ter-bidentate complexes recorded at 10 K in frozen acetonitrile/propionitrile mixture (6/4) or in solid state.

Compound	$\lambda_{emission}$ / nm	$\lambda_{excitation}$ / nm	$\bar{\upsilon}_{excitation}$ / cm^{-1}	Assignment
$[Cr(phen)_3](PF_6)_3$ (**2**)	729	431 [a] 446 [a] 691 [b] 700 [b]	23202 22400 14471 14286	LMCT / $^4[^3(\pi^*\leftarrow\pi)]$ Cr ($^4T_2 \leftarrow {}^4A_2$) Cr ($^2T_1 \leftarrow {}^4A_2$)
$[Cr(phen)_2(phenBr)](PF_6)_3$ (**3**)	729	431 [a] 448 [a] 691 [b] 698 [b]	23202 22321 14471 14327	LMCT / $^4[^3(\pi^*\leftarrow\pi)]$ Cr ($^4T_2 \leftarrow {}^4A_2$) Cr ($^2T_1 \leftarrow {}^4A_2$)
$[Cr(phen)_2(phenAlkyn)](BF_4)_3$ (**6**)	729 731	468 [a] 689 [b] 698 [b,sh]	21368 14514 14327	Cr ($^4T_2 \leftarrow {}^4A_2$) Cr ($^2T_1 \leftarrow {}^4A_2$)
$[Cr(phen)_2(phenNO_2)](CF_3SO_3)_3$ (**7**)	730	433 [a] 485 [b] 684 [b] 692 [b] 702 [b]	23095 20619 14620 14451 14245	LMCT / $^4[^3(\pi^*\leftarrow\pi)]$ Cr ($^4T_2 \leftarrow {}^4A_2$) Cr ($^2T_1 \leftarrow {}^4A_2$)
$[Cr(phen)_2(phenNH_2)](CF_3SO_3)_3$ (**8**)	729	431 [a] 482 [a] 590 [a]	23202 20747 16949	LMCT / $^4[^3(\pi^*\leftarrow\pi)]$ Cr ($^4T_2 \leftarrow {}^4A_2$)
$[Cr(phen)_2(bipy)](BF_4)_3$ (**9**)	729 732	431 [a] 460 [a] 691 [b] 697 [b,sh]	23202 21739 14472 14347	LMCT / $^4[^3(\pi^*\leftarrow\pi)]$ Cr ($^4T_2 \leftarrow {}^4A_2$) Cr ($^2T_1 \leftarrow {}^4A_2$)
$[Cr(phen)_2(dpma)](CF_3SO_3)_3$ (**10**)	747 743	435 [a] 465 [a] 685 [b] 699 [b] 707 [b]	22989 21505 14599 14306 14144	LMCT / $^4[^3(\pi^*\leftarrow\pi)]$ Cr ($^4T_2 \leftarrow {}^4A_2$) Cr ($^2T_1 \leftarrow {}^4A_2$)

Energies are given for the maximum of the band envelope in cm^{-1}. [a] Transitions observed in frozen solution. [b] Transitions observed in the solid state. [sh] Shoulder observed in the solid state.

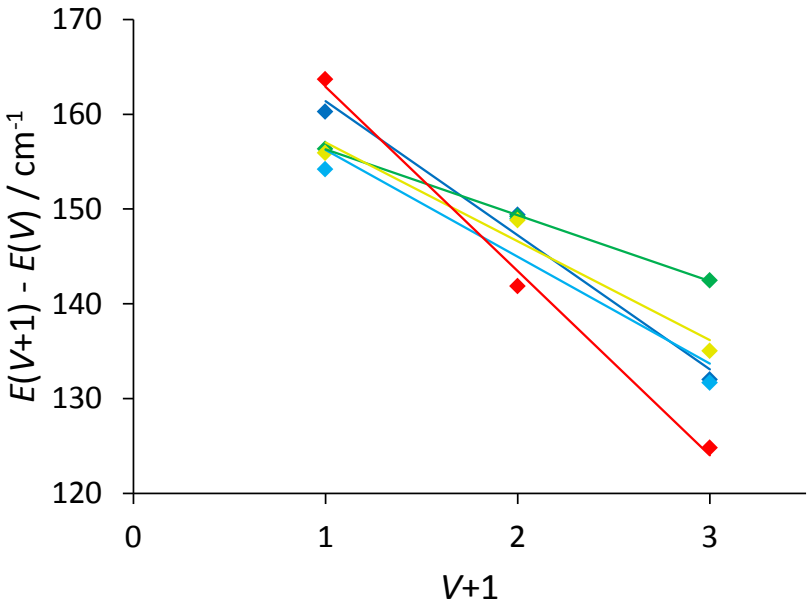

Fig. S34 Plots of energy gaps between two successive vibrational levels in the ground state as a function of the vibronic V+1 level obtained at 10 K for $[Cr(phen)_3](PF_6)_3$ (**2**) (blue), $[Cr(phen)_2(phenBr)](PF_6)_3$ (**3**) (light blue), $[Cr(phen)_2(phenAlkyn)](BF_4)_3$ (**6**) (green), $[Cr(phen)_2(phenNO_2)](CF_3SO_3)_3$ (**7**) (yellow), $[Cr(phen)_2(bipy)](BF_4)_3$ (**9**) (red).

Table S27 Morse potential dissociation energy (D), fundamental frequency (ν_0), and zero point energy $E(V=0) = -D + \frac{h\nu_0}{2}\left(1 - \frac{h\nu_0}{8D}\right)$ for the ground Cr(^{4}E) states computed with eq. (3).

Complexes	D / cm^{-1}	$h\nu_0$ / cm^{-1}	$E(V=0) + D$ / cm^{-1}
$[Cr(phen)_3](PF_6)_3$ (**2**)	1090	176	86
$[Cr(phen)_2(phenBr)](PF_6)_3$ (**3**)	1240	168	82
$[Cr(phen)_2(phenAlkyn)](BF_4)_3$ (**6**)	1920	163	81
$[Cr(phen)_2(phenNO_2)](CF_3SO_3)_3$ (**7**)	1340	167	82
$[Cr(phen)_2(bipy)](BF_4)_3$ (**9**)	855	182	89

Table S28 $Cr(^2E)$ lifetimes of heteroleptic $[CrN_6]$ ter-bidentate complexes measured from 10 K to 300 K (acetonitrile/propionitrile mixture (6/4), $C = 5\times10^{-3}$ mol/L).

Complex	T / K	$\lambda_{emission}$ / nm	τ_1 / ms	τ_2 / ms	A_1	A_2
$[Cr(phen)_3](PF_6)_3$ (**2**)	10	727	2.1(2)	0.23(2)	0.02774	0.01059
	30		1.9(2)	0.18(2)	0.00475	0.00674
	50		2.2(2)	0.15(2)	0.00356	0.00638
	80		2.4(2)	0.16(2)	0.00254	0.0044
	100		1.8(2)	0.20(2)	0.0087	0.01086
	150		1.8(2)	0.19(2)	0.000543	0.00127
	160		0.88(9)	0.10(1)	0.01354	0.02034
	175		0.13(1)		0.1189	
	200		0.047(5)		0.10881	
	250		0.021(2)		0.08397	
	300		0.0079(8)		0.06722	
$[Cr(phen)_2(phenBr)](PF_6)_3$ (**3**)	10	730	1.7(2)	0.22(2)	0.00731	0.00565
	50	730	1.4(1)	0.16(2)	0.00127	0.00471
	100	730	1.55(15)	0.13(1)	0.0057	0.02032
	150	730	1.9(2)	0.082(8)	0.0081	0.04764
	170	730	0.13(1)		0.03819	
	200	726	0.055(6)		0.07059	
	250	726	0.029(3)		0.06214	
	300	726	0.0092(9)		0.05376	
$[Cr(phen)_2(phenAlkyn)](BF_4)_3$ (**6**)	10	729	2.9(3)	0.60(6)	0.0056	0.00315
	50	729	3.6(4)	0.19(2)	0.00141	0.0017
	100	727	3.5(4)	0.19(2)	0.00127	0.00129
	150	726	3.5(4)	0.13(1)	0.00125	0.00113
	160	726	3.1(3)	0.063(6)	0.00143	0.00334
	170	726	0.092(9)		0.04501	
	200	726	0.028(3)		0.03237	
	250	726	0.013(1)		0.02477	
	300	726	0.0069(7)		0.01787	
$[Cr(phen)_2(phenNO_2)](CF_3SO_3)_3$ (**7**) [a]	10	728	1.4(1)	0.18(2)	0.00554	0.0083
	20		1.0(1)	0.13(1)	0.00584	0.00912
	50		0.48(5)	0.053(5)	0.01439	0.01973
	100		0.39(4)	0.058(6)	0.02123	0.03111
	150		0.30(3)	0.033(3)	0.03614	0.04809
	200		0.25(3)	0.028(3)	0.03715	0.05107
	250		0.28(3)	0.027(3)	0.02852	0.04676
	300		0.17(2)	0.016(2)	0.02431	0.03669

$[Cr(phen)_2(phenNH_2)](CF_3SO_3)_3$ (**8**)	10	729	0.37(4)	0.030(3)	0.00014399	0.0003312
	50	729	0.34(3)	0.026(3)	0.00006619	0.0001906
	100	729	0.10(1)	0.0059(6)	0.00006374	0.0002453
	150	729	0.026(3)	0.00088(9)	0.00006717	0.0004325
	200	729	0.0048(5)	0.00019(2)	0.0009987	0.00236
	250	700	0.0019(2)	0.00019(2)	0.0005405	0.00365
	300	700	0.00086(9)	0.00009(1)	0.0009197	0.00918
$[Cr(phen)_2(bipy)](BF_4)_3$ (**9**)	10	729	3.0(3)		0.00305	
	15	727	2.6(3)	0.61(6)	0.0016	0.00257
	20	727	1.4(1)	0.23(2)	0.00403	0.00506
	30	727	1.4(3)	0.20(2)	0.00194	0.00574
	50	727	0.67(7)	0.10(1)	0.00137	0.00460
	70	727	0.69(7)	0.081(8)	0.00106	0.00463
	100	727	0.68(7)	0.070(7)	0.00129	0.0063
	150	727	0.28(3)	0.044(4)	0.00148	0.00555
	170	727	0.073(7)		0.0274	
	200	727	0.023(2)		0.0362	
	300	727	0.0089(9)		0.02674	
$[Cr(phen)_2(dpma)](CF_3SO_3)_3$ (**10**)	10	747	1.4(1)	0.13(1)	0.02794	0.01298
	50	747	1.2(1)	0.18(2)	0.02383	0.0122
	100	747	1.3(1)	0.22(2)	0.01546	0.01056
	150	743	1.4(1)	0.14(1)	0.00719	0.00852
	160	743	0.62(6)	0.084(8)	0.0069	0.01448
	170	743	0.032(3)		0.08911	
	180	743	0.018(2)		0.08705	
	200	743	0.0096(9)		0.0852	
	250	743	0.0034(3)		0.06931	
	300	743	0.0011(1)		0.01589	

Bi-exponential decay were observed until melting point (150 K) due to some aggregates formation during the freezing process. Intensity decay curves were fitted with the following equation: $I = A_1 e^{-\frac{t}{\tau_1}} + A_2 e^{-\frac{t}{\tau_2}} + y_0$, where τ_1 stands for isolated solvated complex, and τ_2 reflects characteristic lifetimes of aggregates, in which quenching processes *via* energy transfer process occurs.[80,38] *a* Measured in the solid state due to degradation in propionitrile.

Table S29 Cr(^{2}E) lifetimes of heteroleptic CrN_6 ter-bidentate complexes measured in freeze pump thaw degassed acetonitrile solution (293 K, $C = 10^{-4}$ mol/L).

Complex	λ_{em} / nm	τ_1 / μs	τ_2 / μs	A_1	A_2
$[Cr(phen)_3](PF_6)_3$ (**2**)	726	224	-	0.00298	-
$[Cr(phen)_2(phenBr)](PF_6)_3$ (**3**)	726	214	-	0.00723	-
$[Cr(phen)_2(phenAlkyn)](BF_4)_3$ (**6**)	726	259	-	0.00672	-
$[Cr(phen)_2(phenNO_2)](CF_3SO_3)_3$ (**7**)	726	177	-	0.0034	-
$[Cr(phen)_2(phenNH_2)](CF_3SO_3)_3$ (**8**)	726	17	0.75	0.00222	0.00297
$[Cr(phen)_2(bipy)](BF_4)_3$ (**9**)	726	208	-	0.00679	-
$[Cr(phen)_2(dpma)](CF_3SO_3)_3$ (**10**)	743	23	-	0.00343	-

Mono-exponential decay were observed for all complexes excepted $[Cr(phen)_2(phenNH_2)](CF_3SO_3)_3$ (**8**) which showed a bi-exponential decay. Intensity decay curves were fitted with following equation: $I = A_1 e^{-\frac{t}{\tau_1}} + A_2 e^{-\frac{t}{\tau_2}} + y_0$.

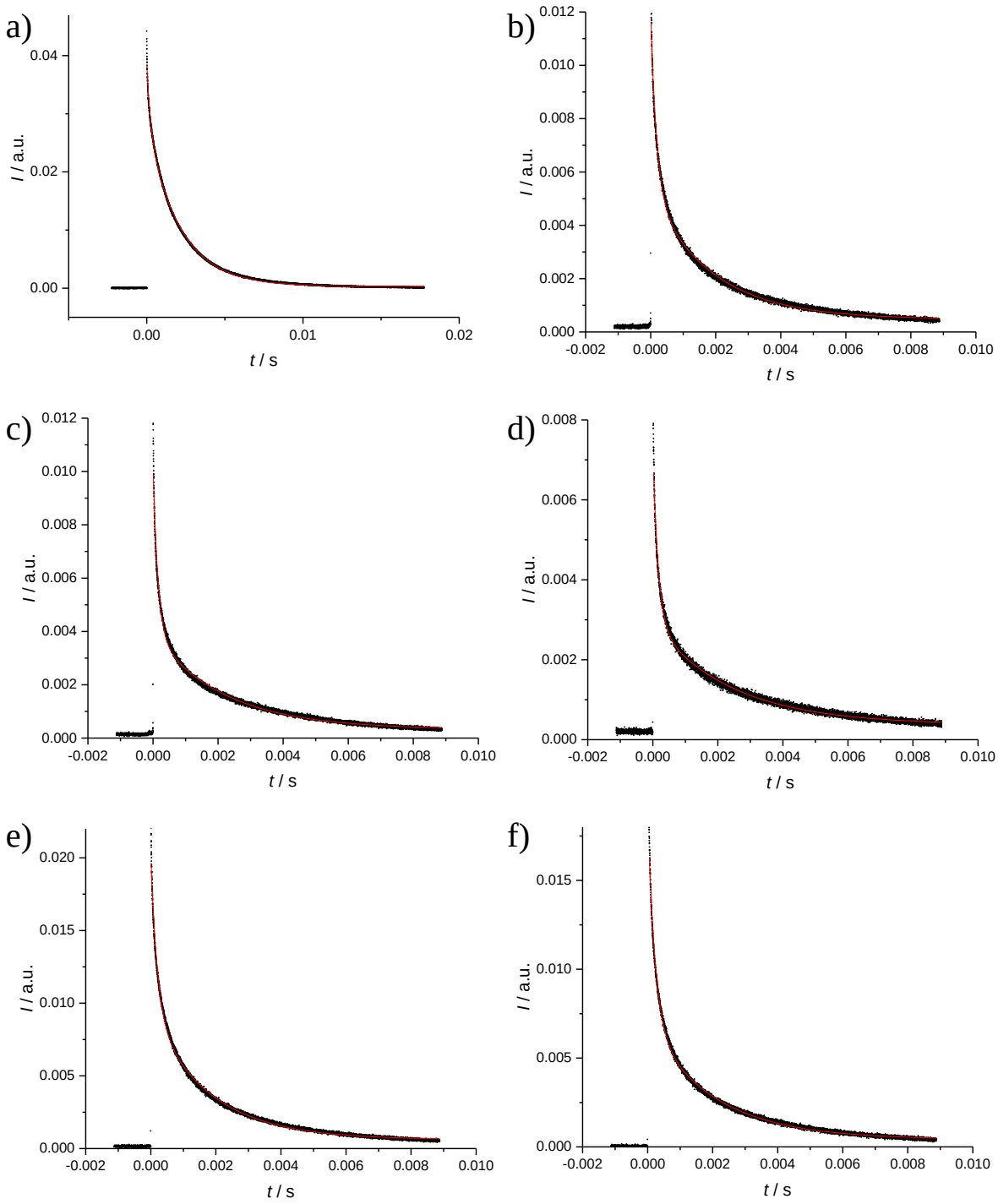

Fig. S35 Luminescence decay curves of $[Cr(phen)_3](PF_6)_3$ (**2**) in acetonitrile/propionitrile (6/4), $C = 5\times10^{-3}$ mol/L, (λ_{exc} = 355 nm, λ_{em} = 727 nm) at a) 10 K, b) 30 K, c) 50 K, d) 80 K, e) 100 K, f) 150 K. Experimental data (black dots), double exponential least squares fits (red line).

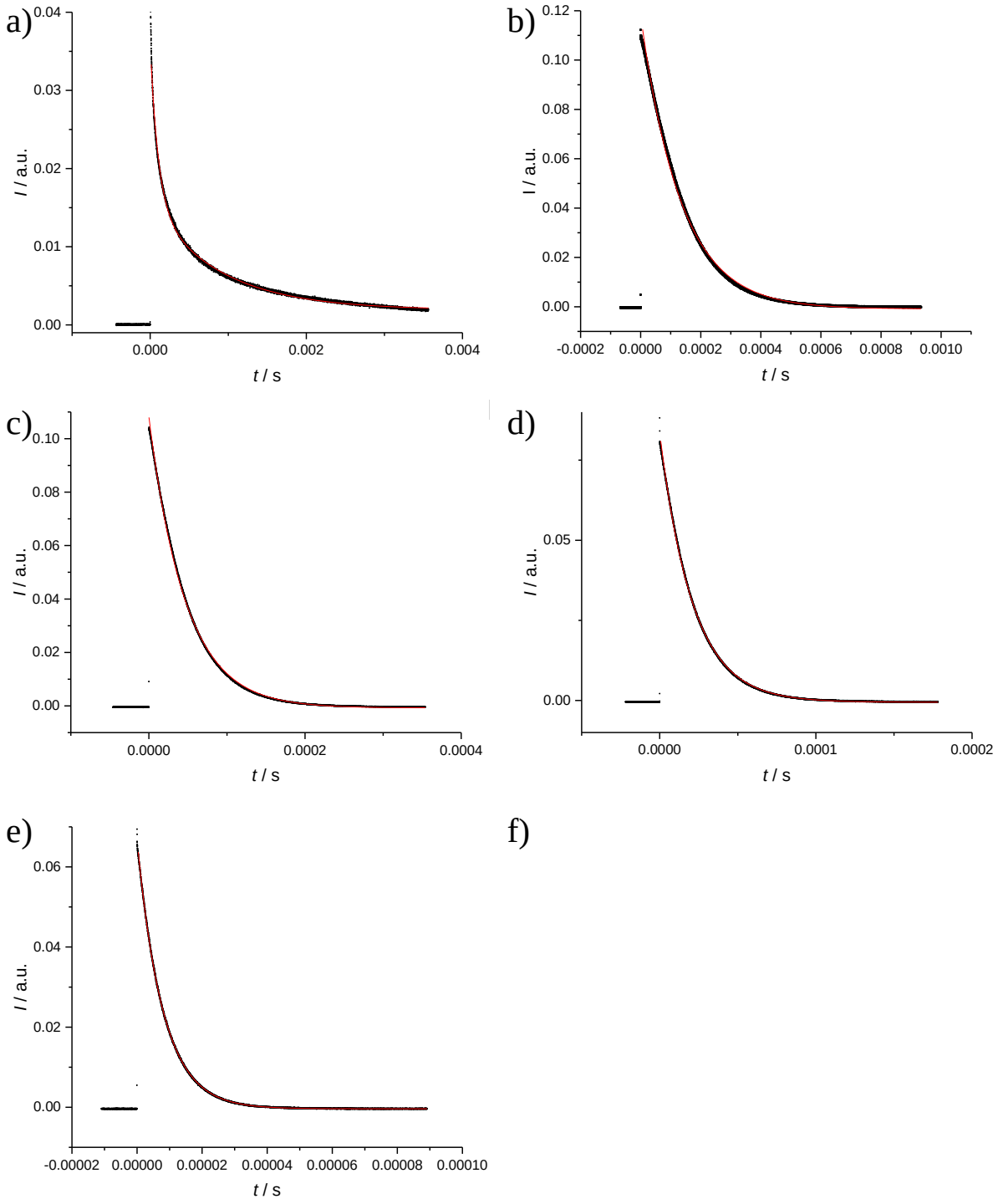

Fig. S36 Luminescence decay curves of $[Cr(phen)_3](PF_6)_3$ (**2**) in acetonitrile/propionitrile (6/4), $C = 5\times10^{-3}$ mol/L, (λ_{exc} = 355 nm, λ_{em} = 727 nm) at a) 160 K, b) 175 K, c) 200 K, d) 250 K, e) 300 K. Experimental data (black dots), double exponential least squares fits (red line).

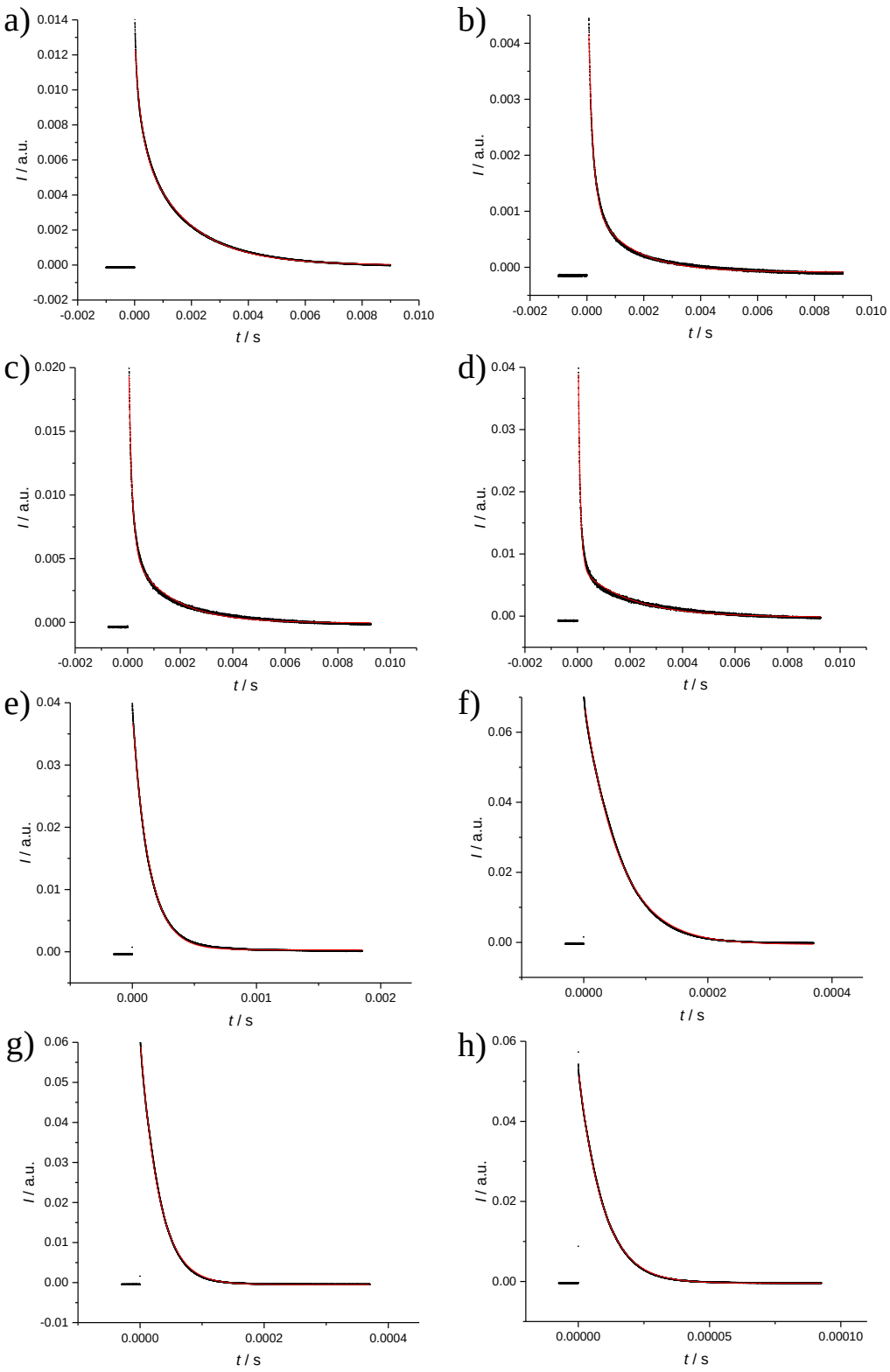

Fig. S37 Luminescence decay curves of $[Cr(phen)_2(phenBr)](PF_6)_3$ (**3**) in acetonitrile/propionitrile (6/4), $C = 5\times10^{-3}$ mol/L, (λ_{exc} = 355 nm) at a) 10 K (λ_{em} = 730 nm), b) 50 K (λ_{em} = 730 nm), c) 100 K (λ_{em} = 730 nm), d) 150 K (λ_{em} = 730 nm), e) 170 K (λ_{em} = 730 nm), f) 200 K (λ_{em} = 726 nm), g) 250 K (λ_{em} = 726 nm), h) 300 K (λ_{em} = 726 nm), Experimental data (black dots), double exponential least squares fits (red line).

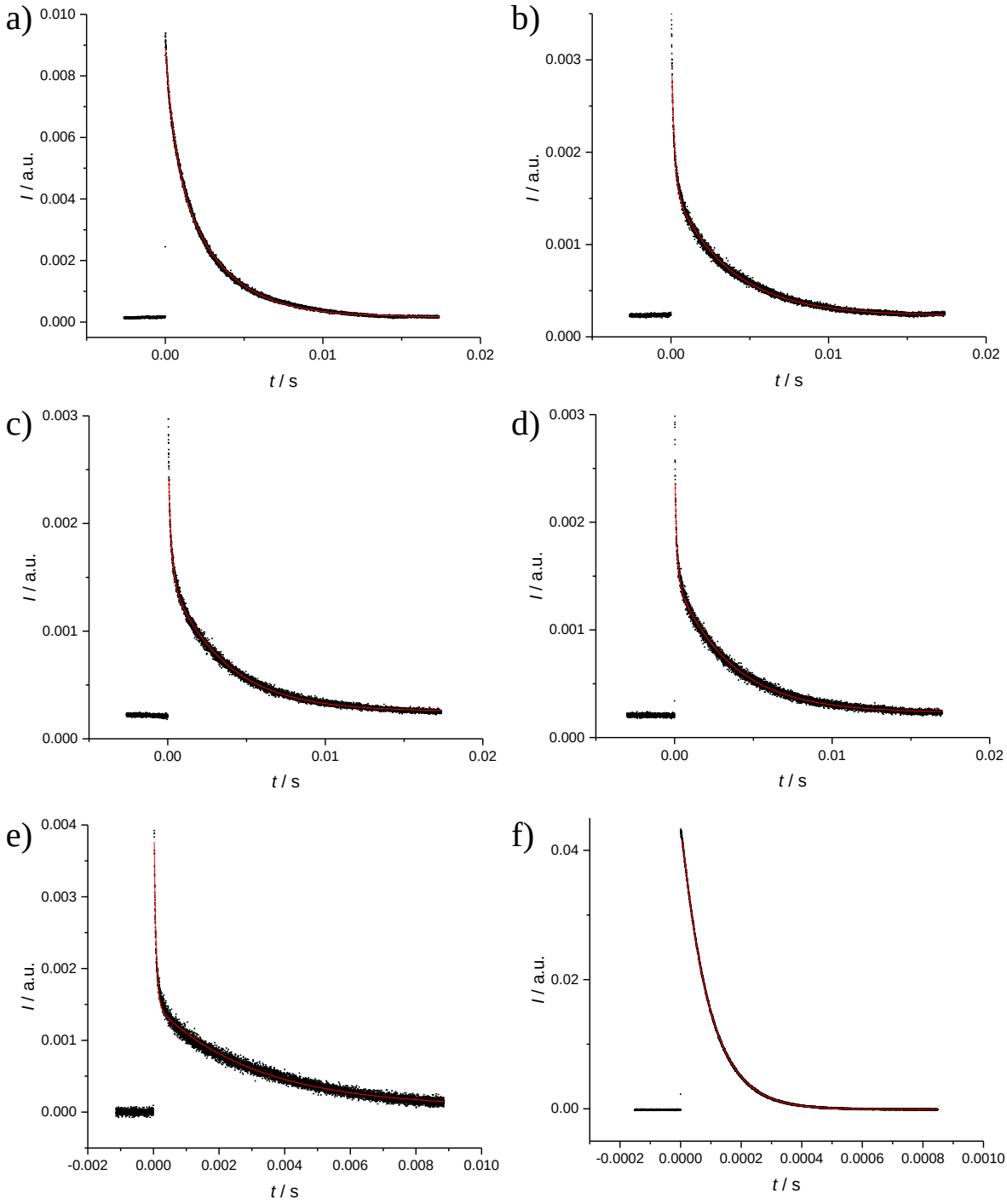

Fig. S38 Luminescence decay curves of $[Cr(phen)_2(phenAlkyn)](BF_4)_3$ (**6**) in acetonitrile/propionitrile (6/4), $C = 5\times10^{-3}$ mol/L, (λ_{exc} = 355 nm) at a) 10 K (λ_{em} = 729 nm), b) 50 K (λ_{em} = 729 nm), c) 100 K (λ_{em} = 727 nm), d) 150 K (λ_{em} = 726 nm), e) 160 K (λ_{em} = 726 nm), f) 170 K (λ_{em} = 726 nm). Experimental data (black dots), double exponential least squares fits (red line).

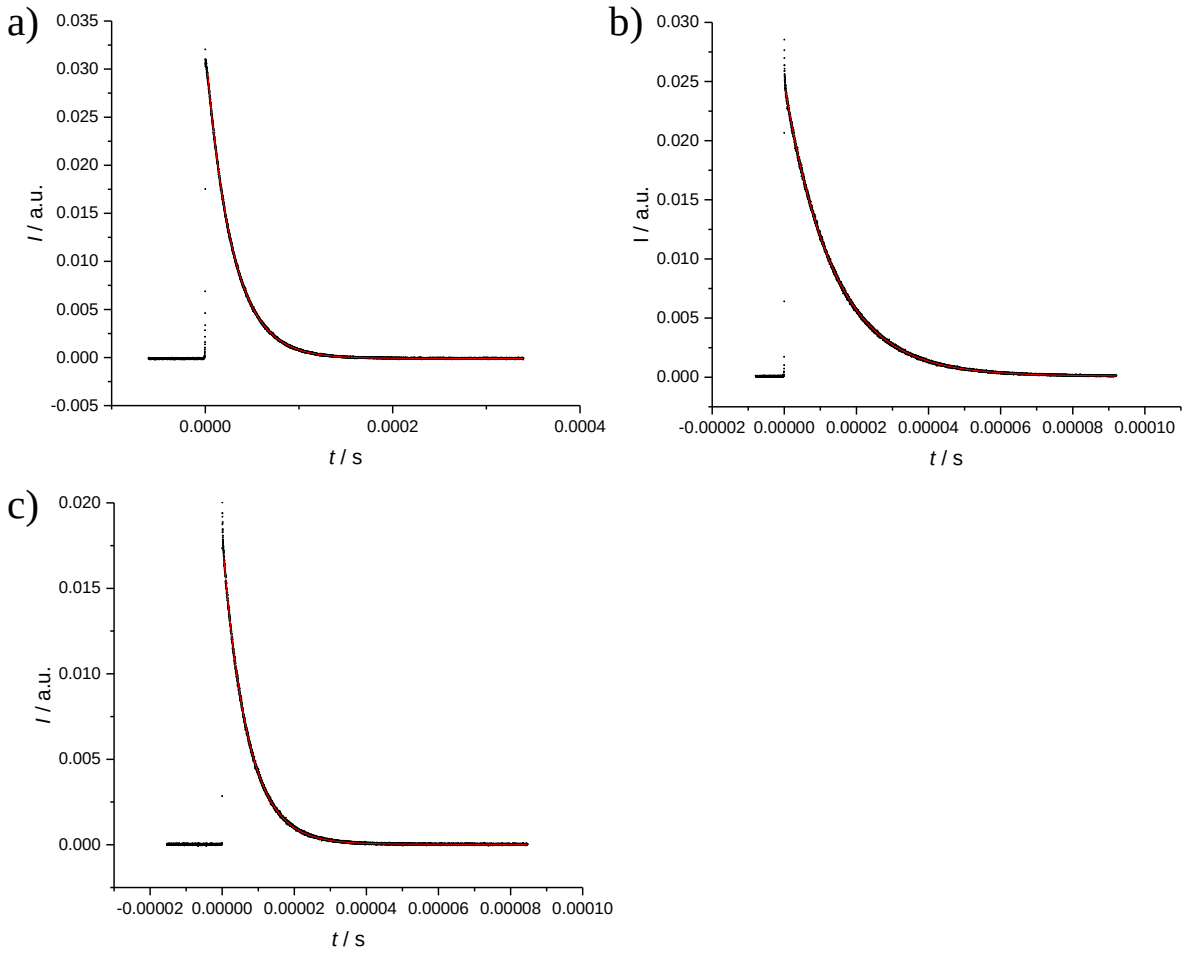

Fig. S39 Luminescence decay curves of $[Cr(phen)_2(phenAlkyn)](BF_4)_3$ (**6**) in acetonitrile/propionitrile (6/4), $C = 5\times10^{-3}$ mol/L, (λ_{exc} = 355 nm) at a) 200 K (λ_{em} = 726 nm), b) 250 K (λ_{em} = 726 nm), c) 300 K (λ_{em} = 726 nm). Experimental data (black dots), double exponential least squares fits (red line).

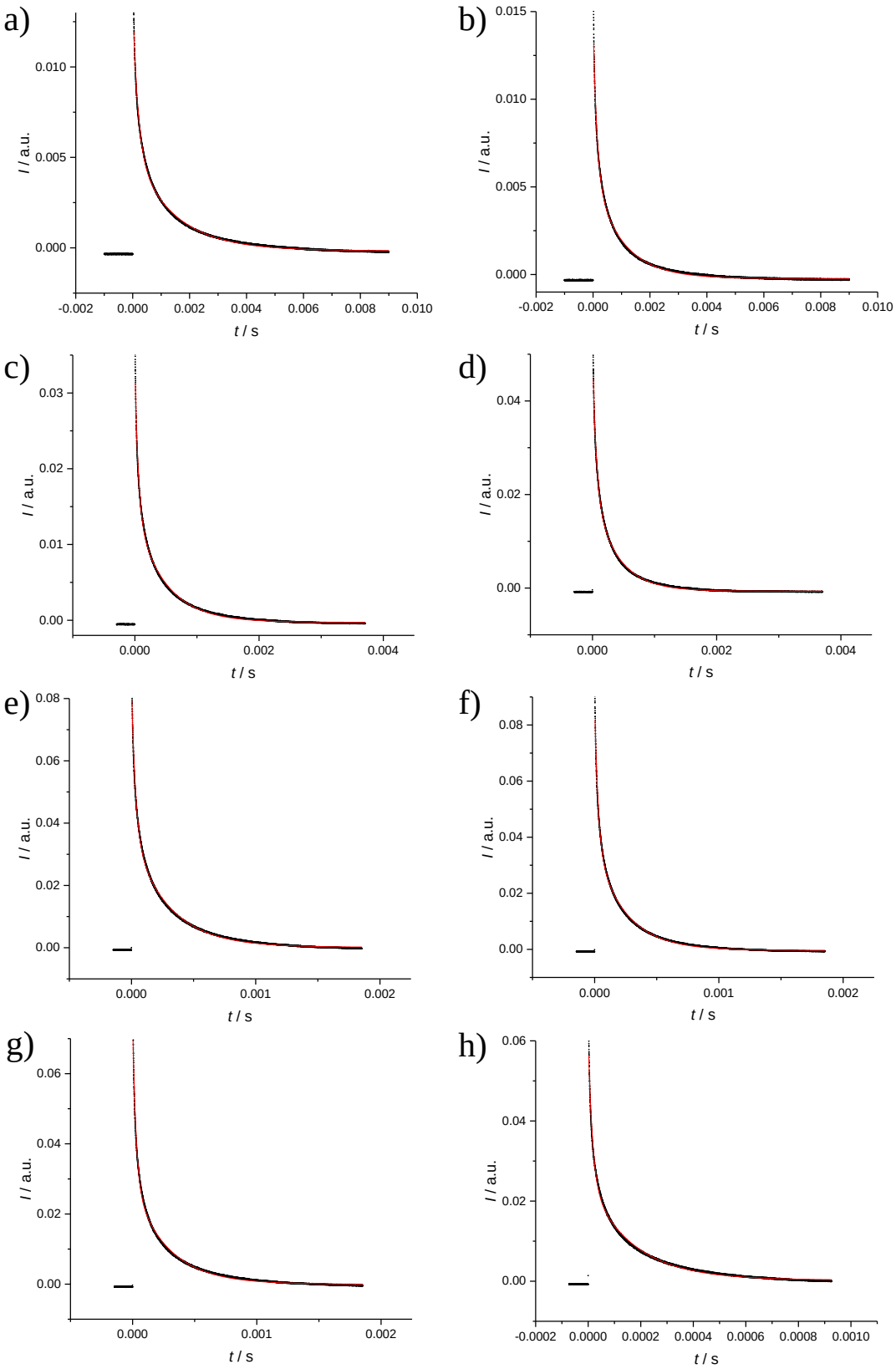

Fig. S40 Luminescence decay curves of $[Cr(phen)_2(phenNO_2)](CF_3SO_3)_3$ (**7**) in the solid state (λ_{exc} = 355 nm, λ_{em} = 730 nm), at a) 10 K, b) 50 K, c) 100 K, d) 150 K, e) 170 K, f) 200 K, g) 250 K, h) 300 K. Experimental data (black dots), double exponential least squares fits (red line).

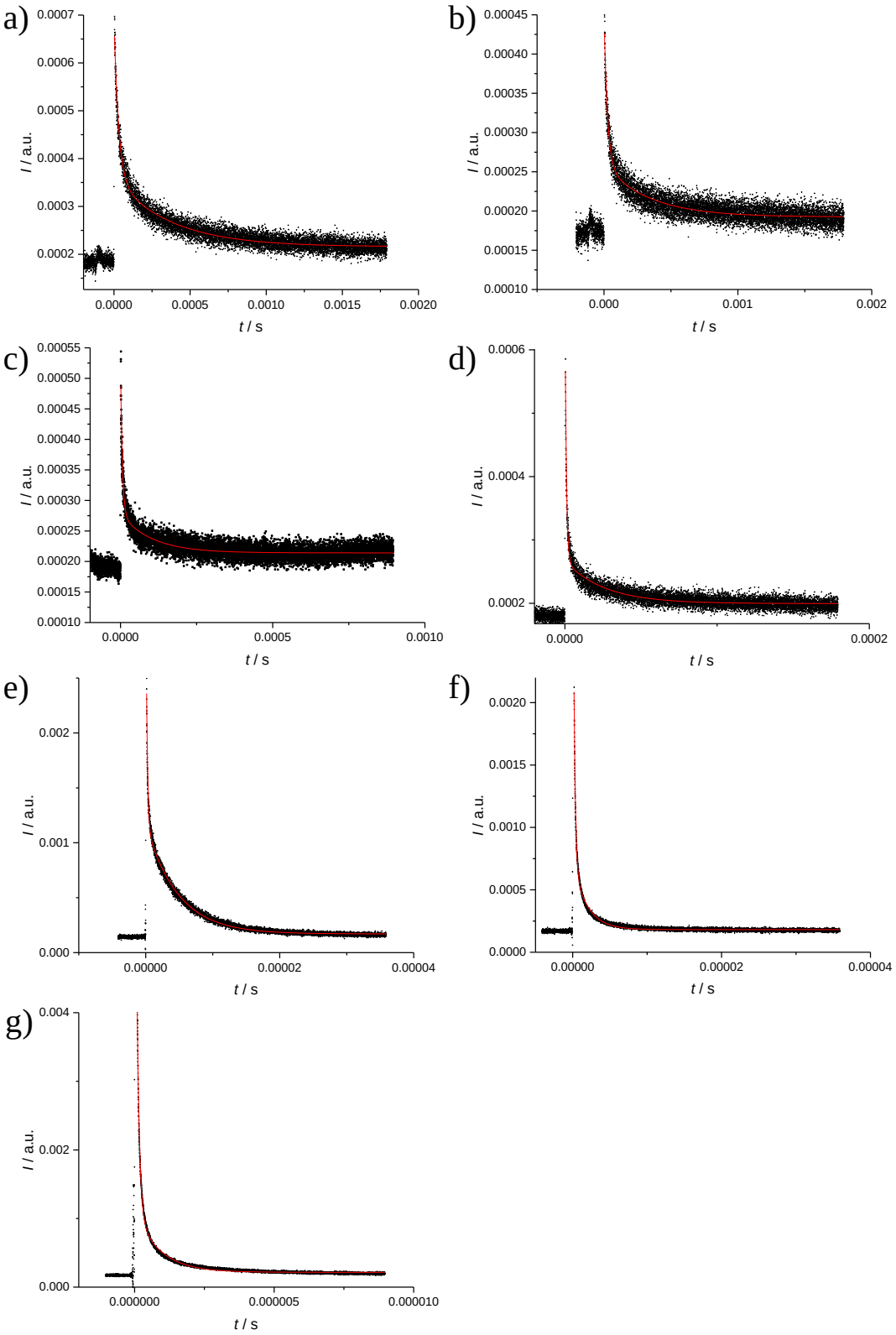

Fig. S41 Luminescence decay curves of $[Cr(phen)_2(phenNH_2)](CF_3SO_3)_3$ (**8**) in acetonitrile/propionitrile (6/4), $C = 5\times10^{-3}$ mol/L, (λ_{exc} = 355 nm) at a) 10 K (λ_{em} = 729 nm), b) 50 K (λ_{em} = 729 nm), c) 100 K (λ_{em} = 729 nm), d) 150 K (λ_{em} = 729 nm), e) 200 K (λ_{em} = 729 nm), f) 250 K (λ_{em} = 700 nm), g) 300 K (λ_{em} = 700 nm). Experimental data (black dots), double exponential least squares fits (red line).

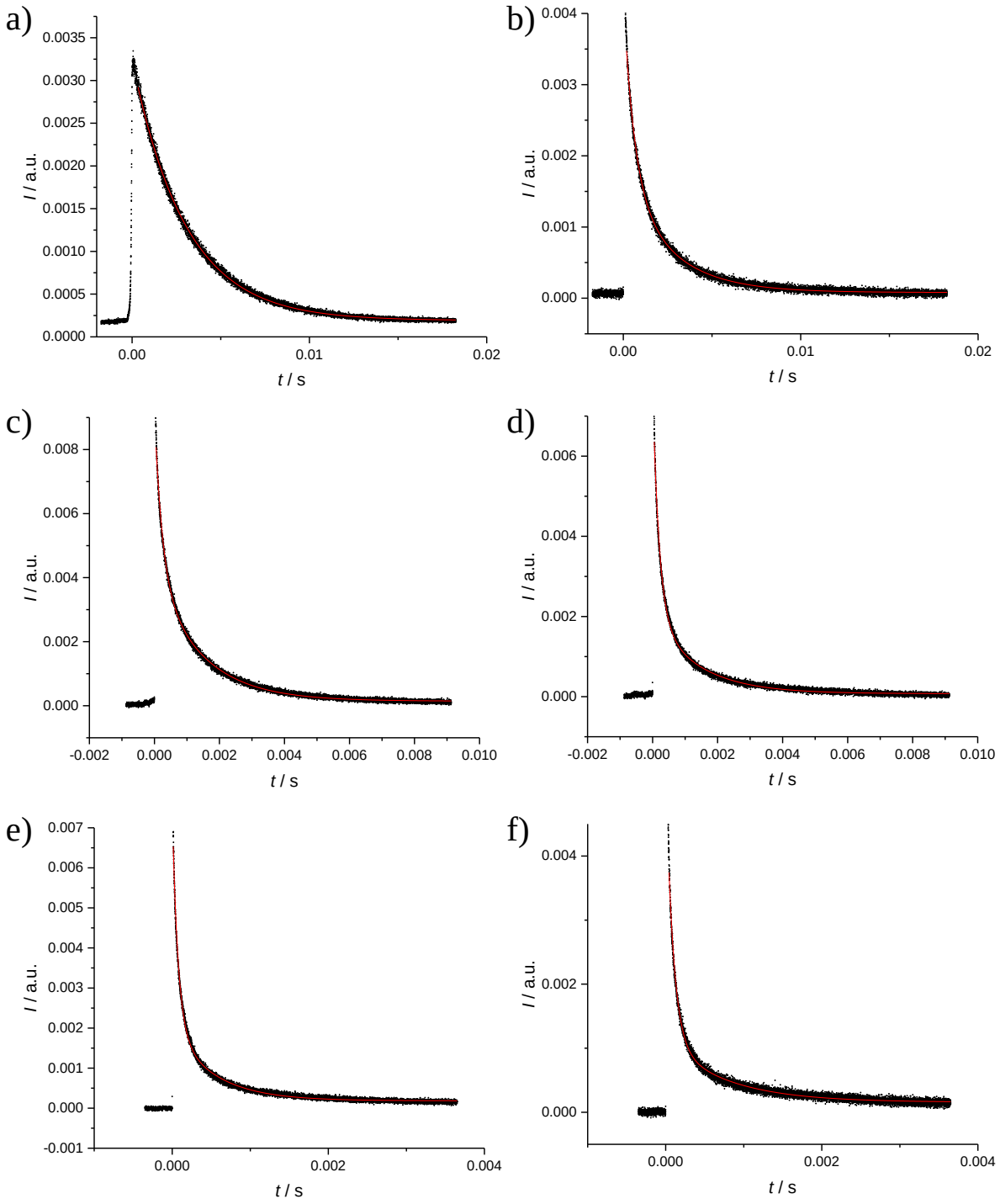

Fig. S42 Luminescence decay curves of $[Cr(phen)_2(bipy)](BF_4)_3$ (**9**) in acetonitrile/propionitrile (6/4), $C = 5\times10^{-3}$ mol/L, (λ_{exc} = 355 nm) at a) 10 K (λ_{em} = 729 nm), b) 15 K (λ_{em} = 727 nm), c) 20 K (λ_{em} = 727 nm), d) 30 K (λ_{em} = 727 nm), e) 50 K (λ_{em} = 727 nm), f) 70 K (λ_{em} = 727 nm). Experimental data (black dots), double exponential least squares fits (red line).

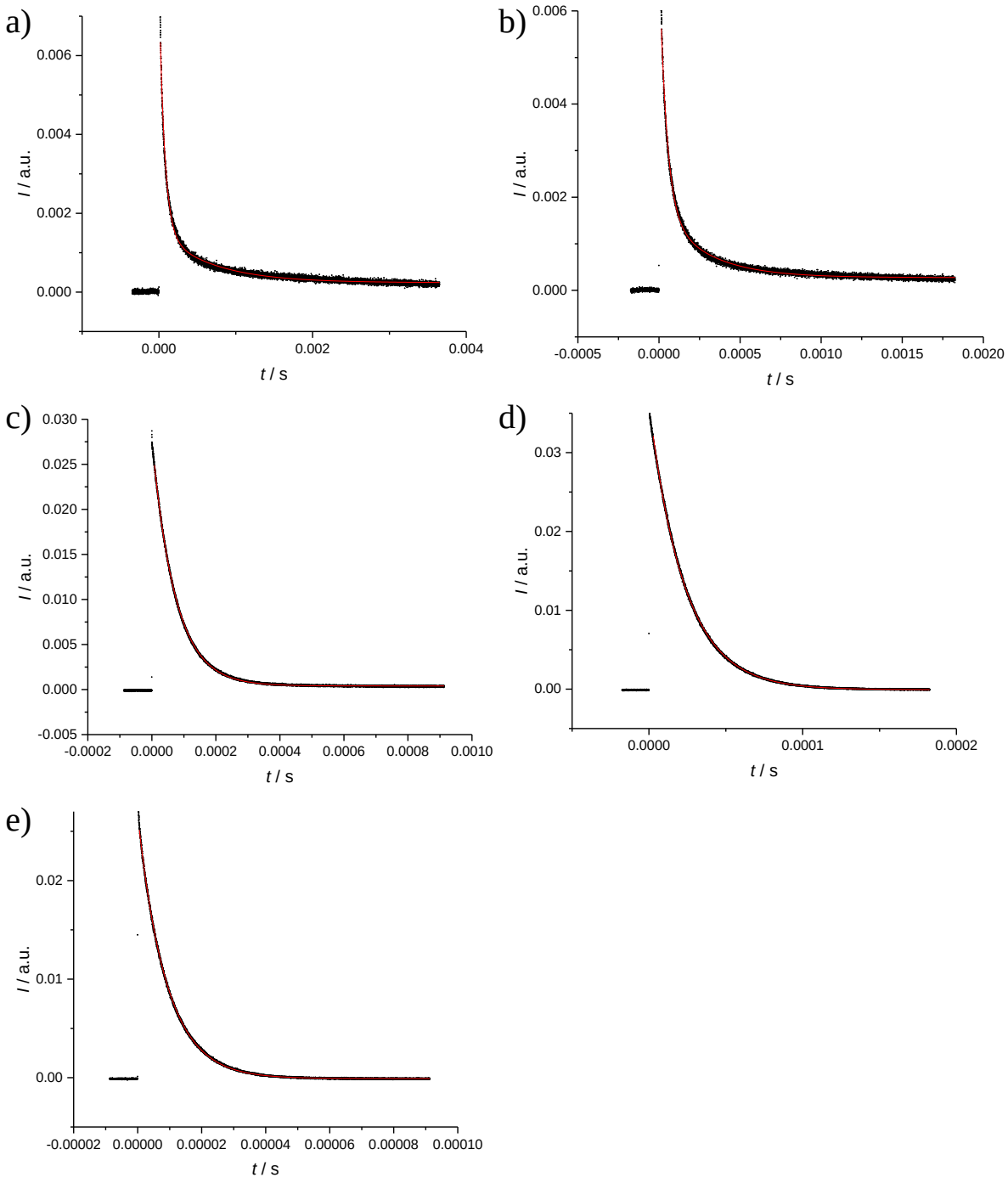

Fig. S43 Luminescence decay curves of $[Cr(phen)_2(bipy)](BF_4)_3$ (**9**) in acetonitrile/propionitrile (6/4), $C = 5\times10^{-3}$ mol/L, (λ_{exc} = 355 nm) at a) 100 K (λ_{em} = 727 nm), b) 150 K (λ_{em} = 727 nm), c) 170 K (λ_{em} = 727 nm), d) 200 K (λ_{em} = 727 nm), e) 300 K (λ_{em} = 727 nm). Experimental data (black dots), double exponential least squares fits (red line).

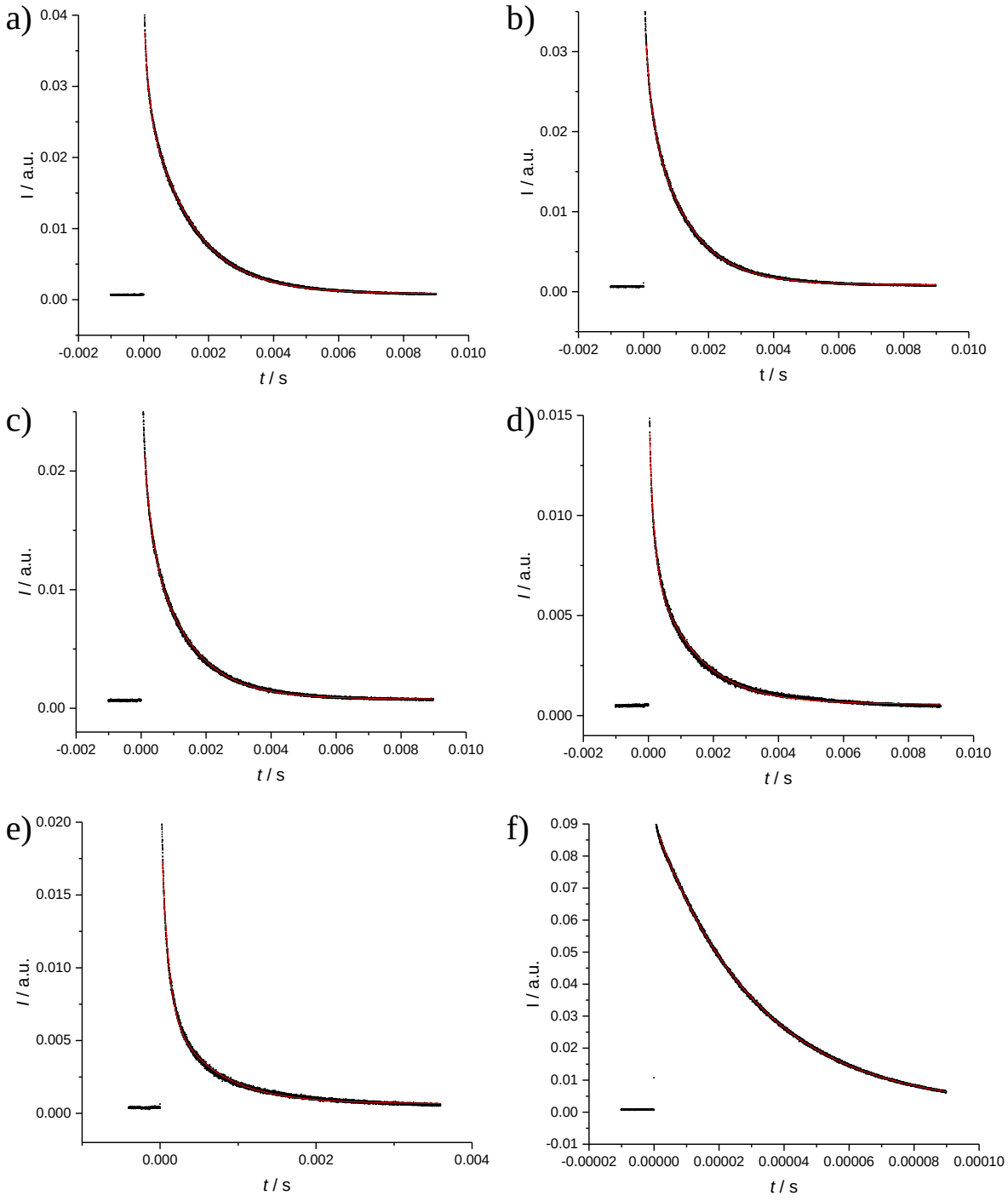

Fig. S44 Luminescence decay curves of $[Cr(phen)_2(dpma)](CF_3SO_3)_3$ (**10**) in acetonitrile/propionitrile (6/4), $C = 5\times10^{-3}$ mol/L, (λ_{exc} = 355 nm) at a) 10 K (λ_{em} = 747 nm), b) 50 K (λ_{em} = 747 nm), c) 100 K (λ_{em} = 747 nm), d) 150 K (λ_{em} = 743 nm), e) 160 K (λ_{em} = 743 nm), f) 170 K (λ_{em} = 743 nm). Experimental data (black dots), double exponential least squares fits (red line).

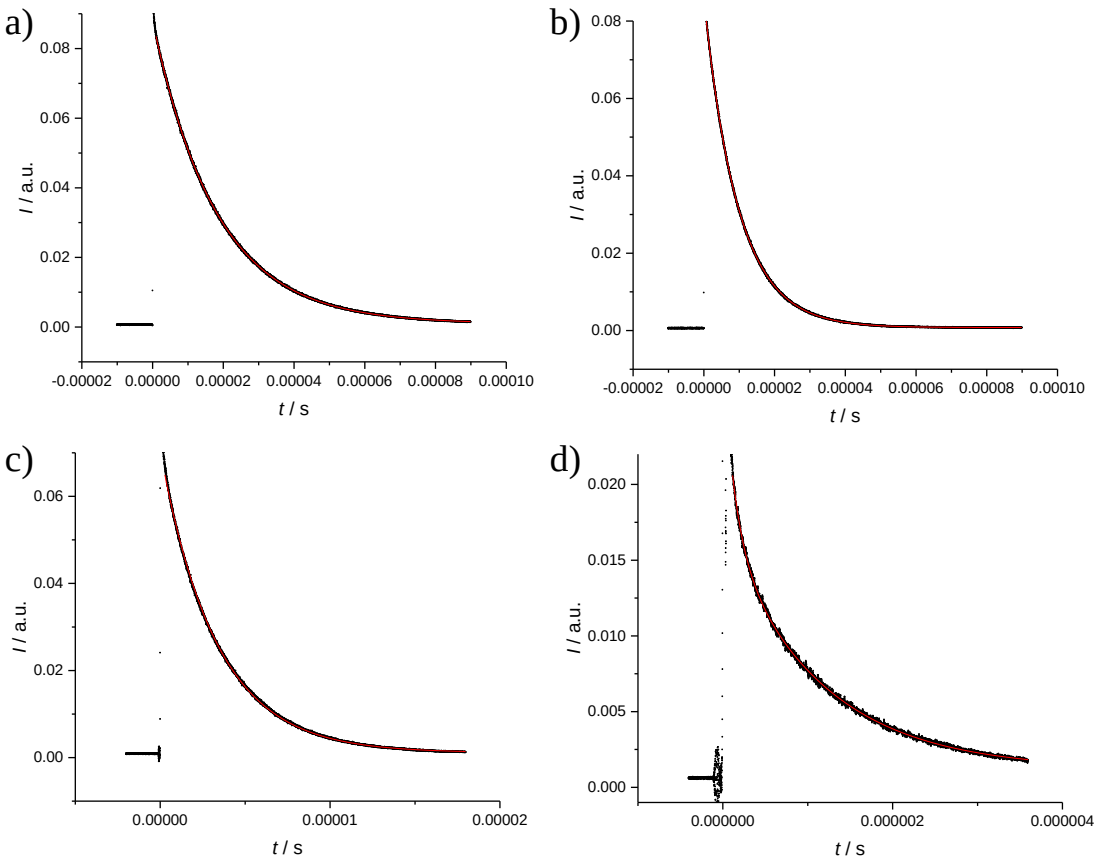

Fig. S45 Luminescence decay curves of $[Cr(phen)_2(dpma)](CF_3SO_3)_3$ (**10**) in acetonitrile/propionitrile (6/4), $C = 5\times10^{-3}$ mol/L, (λ_{exc} = 355 nm) at a) 180 K (λ_{em} = 743 nm), b) 200 K (λ_{em} = 743 nm), c) 250 K (λ_{em} = 743 nm), d) 300 K (λ_{em} = 743 nm). Experimental data (black dots), double exponential least squares fits (red line).

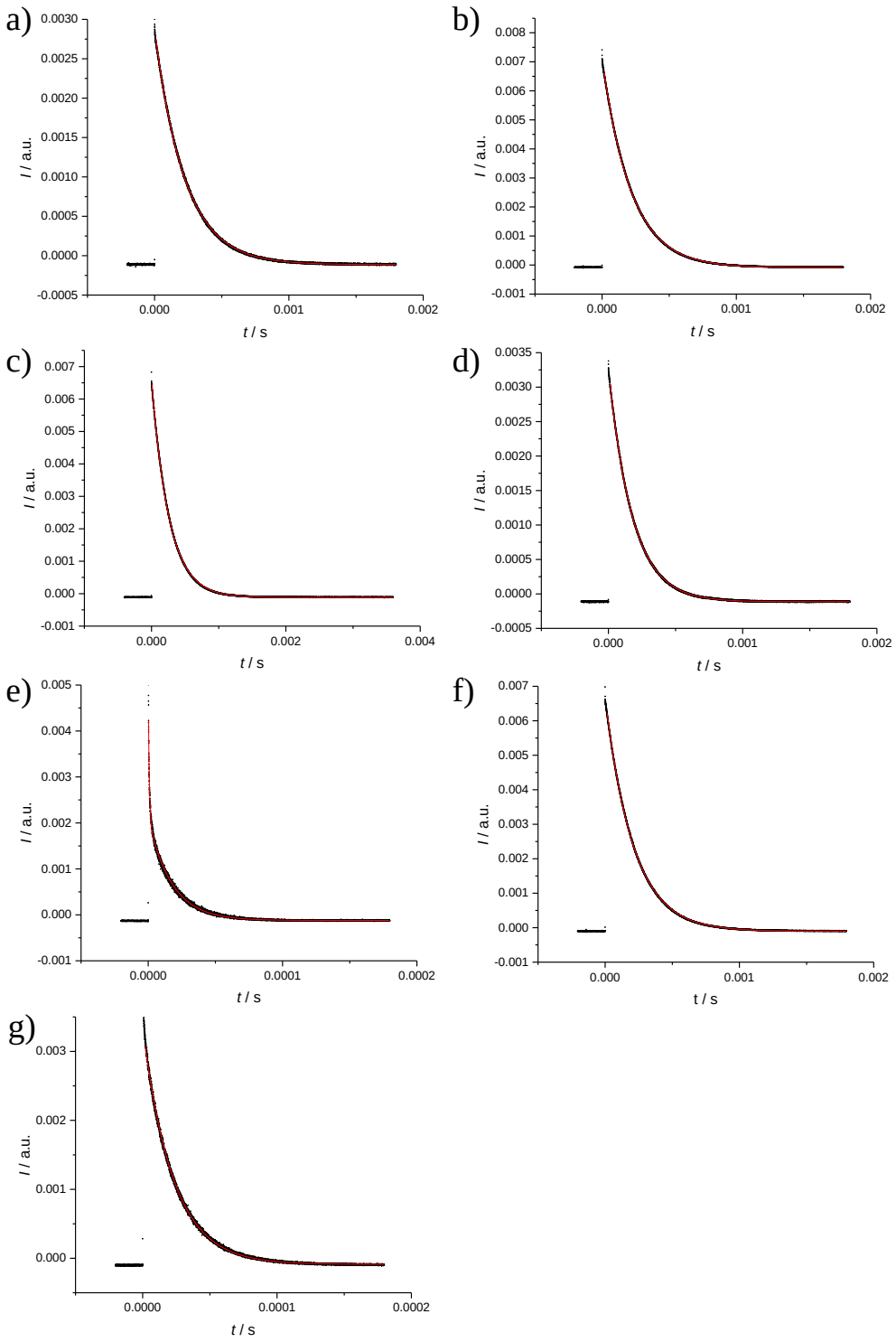

Fig. S46 Luminescence decay curves at 293 K in freeze pump thaw degassed acetonitrile solution (λ_{exc} = 355 nm, C = 10^{-4} mol/L), of a) $[Cr(phen)_3](PF_6)_3$ (**2**) (λ_{em} = 726 nm), b) $[Cr(phen)_2(phenBr)](PF_6)_3$ (**3**) (λ_{em} = 726 nm), c) $[Cr(phen)_2(phenAlkyn)](BF_4)_3$ (**6**) (λ_{em} = 726 nm), d) $[Cr(phen)_2(phenNO_2)](CF_3SO_3)_3$ (**7**) (λ_{em} = 726 nm), e) $[Cr(phen)_2(phenNH_2)](CF_3SO_3)_3$ (**8**) (λ_{em} = 726 nm), f) $[Cr(phen)_2(bipy)](BF_4)_3$ (**9**) (λ_{em} = 726 nm), g) $[Cr(phen)_2(dpma)](CF_3SO_3)_3$ (**10**) (λ_{em} = 743 nm). Experimental data (black dots), exponential least squares fits (red line).

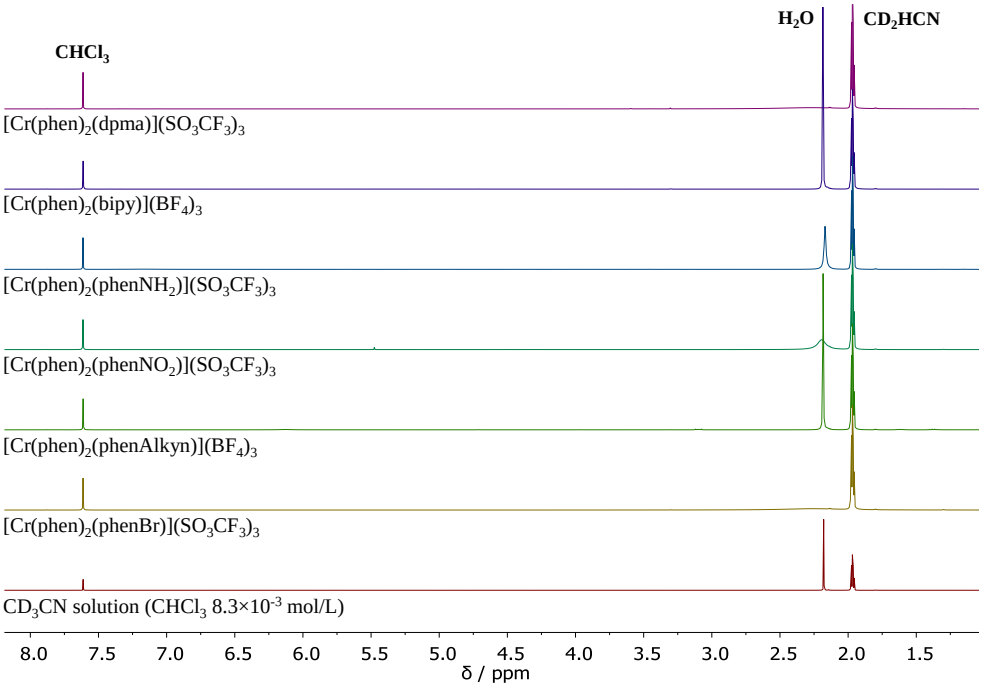

Fig. S47 ^{1}H NMR (400 MHz, CD_3CN) spectra of complexes for the estimation of water amount in solid samples

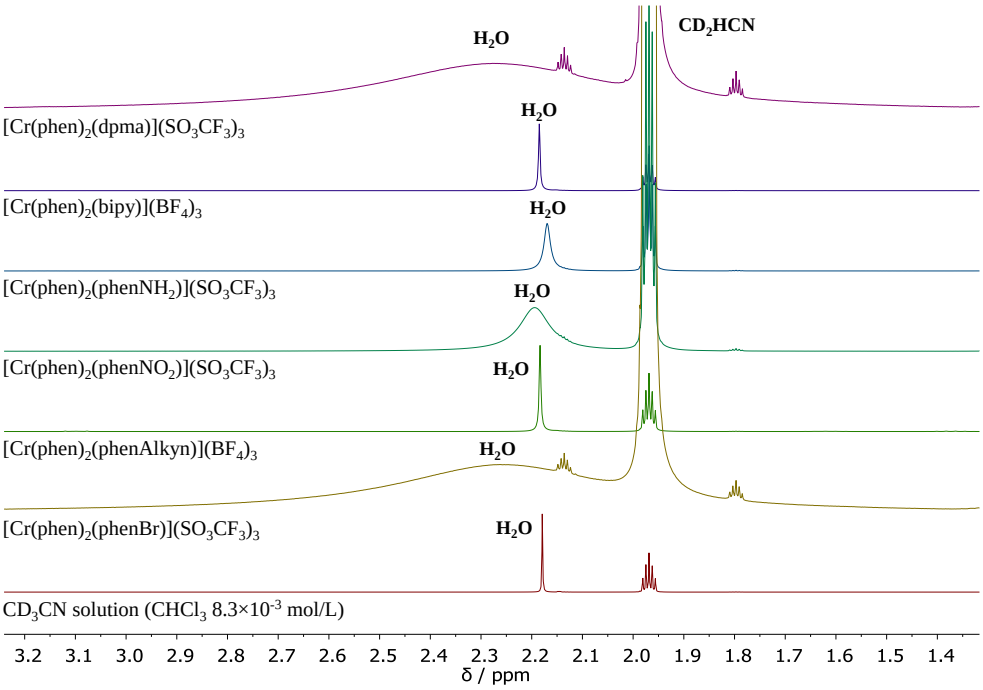

Fig. S48 ^{1}H NMR (400 MHz, CD_3CN) spectra of complexes for the estimation of water amount in solid samples: Zoom on H_2O signal.

Table S30 Number of water molecule (x_{H_2O}) per complex in solid samples of heteroleptic CrN_6 ter-bidentate complexes determined by elemental analysis and by quantitative paramagnetic NMR.

Complex	$x_{H_2O}^{\text{Elemental Analysis}}$	$x_{H_2O}^{\text{NMR } a}$
$[Cr(phen)_2(phenBr)](SO_3CF_3)_3$	2.0(2)	0.5(9)[b]
$[Cr(phen)_2(phenAlkyn)](BF_4)_3$	1.2(2)	1.5(5)
$[Cr(phen)_2(phenNO_2)](CF_3SO_3)_3$	2.5(2)	1.9(5)
$[Cr(phen)_2(phenNH_2)](CF_3SO_3)_3$	1.5(2)	2.0(5)
$[Cr(phen)_2(bipy)](BF_4)_3$	1.3(2)	1.9(5)
$[Cr(phen)_2(dpma)](CF_3SO_3)_3$	0.35(10)	0.5(4)[b]

[a] The amount of water was determined using $CHCl_3$ as an internal reference (8.3×10^{-3} mol/L). The spectrum of the pure solvent was recorded to substract the amount of water brought by the solvent itself or the CD_2HCN contribution in case of overlap with the water signal. Important errors should be considered due to large proportion of water coming from the solvent (around 90%) compared with that relaxed by the complex (around 10 %). [b] For those two complexes the broadness of the water signal induces severe overlap with the CD_2HCN multiplet.